Ionic Radii in Aqueous Solutions

YIZHAK MARCUS

Department of Inorganic and Analytical Chemistry, The Hebrew University of Jerusalem, 91904 Jerusalem, Israel

Received February 1, 1988 (Revised Manuscript Received April 20, 1988)

Contents

I. Introduction

In many studies of electrolyte solutions the concept of "ionic radius" plays an important, sometimes even a dominant, role. Most properties of such solutions, including thermodynamic, transport, spectroscopic, and other properties, depend in one manner or another on the ability of solvent or other solute particles to approach a given ion and on their distance-dependent interactions with it. Most authors employ for this purpose, without thinking it necessary to justify this, the "crystal ionic radii" of ions. These quantities may, indeed, characterize the ions in crystalline ionic solids and commonly are considered to be inherent properties of them (but see section III.A).

It is, however, not self-evident that these quantities are valid as descriptors of the ions in general, in gaseous as well as in liquid phases, and in particular in electrolyte solutions. For instance, it has been argued by Stokes[1] that for ions in the gaseous phase the radii that are relevant for their hydration energies are their van der Waals, rather than their crystal ionic, radii. Conversely, it has been argued by Rashin and Honig[2] that (for the alkali-metal cations) the covalent radii are the relevant ones. Referring back to the usually employed crystal ionic radii, only if their validity for expressing the radii of the ions in solution is demonstrated for a wide variety of ions on the basis of experimental evidence can the implicit assumption of the validity of the use of crystal ionic radii in lieu of the solution ionic radii be maintained.

Yizhak Marcus was born in Kolberg, Germany, in 1931 and immigrated to Israel in 1936. He obtained his M.Sc. and Ph.D. degrees in 1952 and 1956 from The Hebrew University of Jerusalem. He returned after postdoctoral research in Sweden and the U.S. to the Soreq Nuclear Research Center in Israel in 1958 to work on the actinides and on ion exchange and solvent extraction separations. On this appointment in 1965 as Professor at The Hebrew University, he served until 1973 as Head of the Inorganic and Analytical Chemistry Department. His research interests range from molten salts, through aqueous, nonaqueous, and mixed electrolyte solutions, to mixtures of organic liquids. He has published some 160 research papers and three books on ion exchange and solvent extraction (with A. S. Kertes), on liquid-state chemistry, and on ion solvation. He has served as a visiting professor in universities in Germany, Japan, and the U.S. He is holding a Senior Alexander von Humboldt Fellowship (1971–1976, 1988), and has served on IUPAC bodies in various capacities since 1963.

In fact, several authors have compared experimental evidence that they had obtained on a particular electrolyte solution concerning the distance between the center of an ion and that of the oxygen atom of the nearest water molecules with the sum of the crystal ionic radius of the ion and the "radius" of a water molecule. They then stated that the agreement they observed between these two distances validated their results. Attempts at a generalization of this finding have recently been made by the present author.[3,4] This review substantiates this contention further, by an exhaustive examination of the relevant literature.

Studies are deemed to be relevant if they report numerical values for the distance between a specified ion and the nearest atom belonging to a surrounding solvent molecule in a solution. Many experimental studies on the structure of electrolyte solutions do not answer this

0009-2665/88/0788-1475$06.50/0

criterion: they may report distances inside complexes in solution (central atom–ligand distances), distances involving unspecified hydrolysis products, the number of nearest solvent molecules without giving a distance, etc. Such studies, although of great interest in themselves, are not considered in this review. The literature has been examined till the end of 1986.

II. Some Uses of Ionic Radii in Solution

Many phenomena depend on the ability of other particles to approach an ion in solution. These include ion–solvent, ion–ion, and ion–nonelectrolyte interactions, giving rise to thermodynamic, kinetic, spectroscopic, and other properties of systems that involve ions in solution. In many cases is it possible to relate the phenomena to the radius of the "bare" ion in the solution, i.e., to the radius of the ion without any of its solvation shells. In other cases it is the solvated ion, with at least its first solvation shell, that is the unit that is considered, and then the sum of the radius of the bare ion and the diameter of the solvent molecule is the relevant quantity. In general, therefore, the radius of the ion itself, without its solvation shells in the solution is a highly useful and often employed quantity. Following is a brief account of some of the instances where the radii of bare ions, R_{ion}, in solution can be employed.

A. Thermodynamic Quantities

The thermodynamic quantities of solvation are among those that depend strongly on the size of the ion in solution. Many theoretical approaches, ranging from the simplest consideration of the electrostatic contribution to the standard molar Gibbs free energy of solvation, $\Delta_{\text{solv}}G^\circ_{\text{el}}$, in terms of the primitive model and the Born equation to more sophisticated considerations involving the particulate nature of the solvent, dielectric saturation, etc., depend on the radius of the ion. In the primitive model, the ion is considered as a sphere with a point charge in its center and the solvent as a dielectric continuum. According to the Born equation

$$\Delta_{\text{solv}}G^\circ_{\text{el}} = -(N_{\text{Av}}e^2/8\pi\epsilon_0)(1 - 1/\epsilon)z^2/R_{\text{ion}} \qquad (1)$$

where N_{Av} is Avogadro's constant, e the unit charge, ϵ_0 the permittivity of vacuum, ϵ the relative permittivity of the solvent (its dielectric constant), z the charge of the ion, and R_{ion} its radius. A calculation with eq 1 overestimates the absolute value of $\Delta_{\text{solv}}G^\circ_{\text{el}}$ severely, and various modifications have been suggested. The main merit of the primitive model and the Born equation is the indication of how the electrostatic contributions to derivative thermodynamic functions, such as the standard molar enthalpy, entropy, heat capacity, compressibility, etc., of solvation should depend on the properties of the solvent. The model and equation specify that these quantities should depend on the appropriate derivatives of the relative permittivity of the solvent with respect to the temperature and the pressure.

A recent model that considers all these thermodynamic quantities of solvation but takes into account the dielectric saturation near the ion is due to Marcus.[5] A first solvation shell is defined to extend from R_{ion} to $R_{\text{ion}} + \Delta R$, where ΔR itself is a specified function of (the reciprocal of) R_{ion}. In this first shell complete dielectric saturation takes place, and the solvent is translationally immobilized. Only beyond this first shell does eq 1 hold, with the factor $(1 - 1/\epsilon)$ modified appropriately with derivatives of the relative permittivity with respect to the temperature and the pressure to accommodate all the derived thermodynamic functions. Many other models have been suggested, and undoubtedly many more will yet be, but all must take into account the size of the ion in the solution. Many of them, including that of Marcus,[5] consider also the work required to produce a spherical cavity in the solvent for the accommodation of the ion in it, $\Delta_{\text{solv}}G^\circ_{\text{cav}}$. The radius of this cavity is given directly by R_{ion}, so that this further contribution (and its appropriate derivatives with respect to the temperature and the pressure) to the thermodynamic quantities of solvation is also dependent on the radius of the ion in solution.

Yet other ion–solvent interactions that give rise to the partial molar thermodynamic quantities of electrolytes in solution are related to the sizes of the ions in solution. For instance, the partial molar heat capacity at constant pressure and at infinite dilution[6] has been related, similarly to the corresponding quantity of solvation, to R_{ion}. Many treatments of the partial molar volume[7] and entropy[8] of electrolytes at infinite dilution have also been related to R_{ion}.

Ion–Ion interactions at low concentrations but beyond the applicability of the Debye–Hückel limiting law are governed by the extended Debye–Hückel equation, which for the activity coefficient has the familiar form

$$\log \gamma_{\pm} = -A\mu^{1/2}/(1 + Ba\mu^{1/2}) \qquad (2)$$

where A and B are parameters that depend on the temperature and the relative permittivity of the solvent, μ is the ionic strength of the electrolyte solution, and a is a parameter describing the mean diameter of the ions or the mean distance of nearest approach of the ions to each other. This quantity, again, may be interpreted as the sum of the radii R_{ion} of the ions of opposite charge. It is conceded that in many cases this sum produces a value of a that does not give a good fit of the activity coefficients calculated from eq 2 with the theoretical parameters A and B with the experimental values, but then there are many objections to the validity of eq 2 itself.

When ion pairing becomes important, then again the mean distance of approach of the ions to each other is a crucial parameter, in both the Bjerrum and the Fuoss theories. In the Bjerrum theory the expression for the association constant is

$$K_{\text{ass}}/(\text{L mol}^{-1}) = 4000\pi N_{\text{Av}}u^3 \int_2^b t^{-4}\exp(t)\,dt \qquad (3)$$

where $u = |z_+z_-|e^2/4\pi\epsilon_0\epsilon k_{\text{B}}T$, t is an auxiliary variable, k_{B} is the Boltzmann constant, and $b = u/a$ is the limit of integration. As before, a is the distance of nearest approach of the oppositely charged ions, which should equal the sum of their radii in solution, R_{ion}. The Bjerrum theory specifies ions that are within distances $a \le r \le u/2$ of each other to be associated, whether in contact or separated by some solvent. In the Fuoss theory only contact ion pairs are considered, and the expression for the association constant is

$$K_{\text{ass}}/(\text{L mol}^{-1}) = 4000\pi N_{\text{Av}}a^3\exp(b)/3 \qquad (4)$$

It contains the factor $\exp(b)/3$, where at high b values the Bjerrum theory has approximately $\exp(b)/b$. In both theories, however, b, i.e., a quantity proportional to the reciprocal of a, plays a central role.

B. Kinetic and Transport Quantities

The rate of the solvent exchange between the solvation shells of an ion that undergoes mainly electrostatic interactions with them and the bulk of the solvent is governed by the electric field of the ion. That is, the ratio of the charge of the ion to its radius determines this rate: the larger the field strength, the slower the exchange. Even for transition-metal cations the field strength is important in this respect, although the ligand field stabilization plays a role, too.[9]

The rate of complex formation can often be described as the product of an outer-sphere complex formation equilibrium constant and the rate constant for the replacement of a solvent molecule in the inner sphere by the entering ligand. The former quantity, the outer-sphere equilibrium constant, is calculated by eq 4 for a charged ligand or an expression analogous to it, with b replaced by $-U/k_BT$ for an uncharged one, where U is the interaction energy between the metal ion and the ligand.[9] The rate of formation of the outer-sphere ion pair is given, according to Eigen,[10] by

$$k = 4\pi N_{Av} u(D_+D_-)/(\exp(au) - 1) \qquad (5)$$

where $u = |z_+z_-|(e^2/4\pi\epsilon_0\epsilon k_BT)$ as before and D_i is the diffusion coefficient of the designated ion. The rate constant for the dissociation of the outer-sphere ion pair is given by a similar expression, with $-au$ in the exponent in the denominator and an additional factor of $(3/4\pi N_{Av})a^{-3}$ in the numerator. The distance of approach of ligand to cation, a, is thus again involved, hence also R_{ion}.

The rate of movement of ions in solution, be it self-diffusion or mobility in an electric field, also depends on the size of the ion. According to the Nernst–Hartley relation, the limiting (infinite dilution) value of the (self-) diffusion coefficient of an ion, D°_{ion}, is RT/F^2 times its limiting equivalent conductivity, $\lambda^\circ_{\text{ion}}$; hence both phenomena may be discussed in terms of the limiting ionic mobilities $u^\circ_{\text{ion}} = \lambda^\circ_{\text{ion}}/F$, where F is the Faraday constant. The mobilities are related to properties of the solvent and of the ion by the Stokes law expression

$$u^\circ_{\text{ion}} = {}^1\!/_6\pi\eta^\circ R_{\text{St}} \qquad (6)$$

where η° is the viscosity of the solvent and R_{St} is the "Stokes radius" of the ion. This is not necessarily a valid measure of the size of the moving ion in the solution, in particular not for ions with a "bare-ion" radius < 0.25 nm. However, a plot of the Stokes radii of ions against their bare-ion radii (actually, their crystal ionic radii) permitted Nightingale[11] to arrive at a set of radii for the moving ions in solution (their so-called solvated radii). It is thus seen that the bare-ion radii R_{ion} play an important role even in the determination of the "solvated-ion" radii from experimental mobility data.

C. Spectroscopic Quantities

The significance of ionic radii in spectroscopic investigations of solutions of electrolytes can be demonstrated by many instances, of which the following are a few examples.

The chemical shift of the NMR signal of the water protons, δ, depends in the presence of (diamagnetic) ions on their concentration and their natures. The measurable limiting chemical shift per unit concentration at infinite dilution $(d\delta/dc)_{c=0}$ for an electrolyte must be divided into the (additive) ionic contributions for their interpretation in terms of the interactions that take place in the solution. This can be made on the basis of the relative sizes of the ions in the solution.[12] The partially compensating negative shift due to the electrostatic field of the ion and a positive shift due to the breaking of the hydrogen bonds in the solvent by it can then be evaluated for each ion. The former effect is thus proportional to the reciprocal of the ionic radius, and the latter effect to the volume of the ion, i.e., to the third power of its radius.[13] The NMR line widths, from which the rates of relaxation of the solvent molecules in the solvation can be evaluated, are less sensitive to the sizes of the ions.

The ultraviolet charge transfer to solvent spectra of anions in various solvents have been interpreted in terms of the "confined model", according to which the anion is located in a square potential well of a definite radius.[14] This radius depends on the radius of the anion in the solution, with added terms for the penetration distance of the electron into the solvent and the free space between the ion and the solvent. The latter quantity is temperature dependent and can be eliminated by extrapolation to absolute zero, whereas the former added term is solvent dependent but ion independent. Thus the knowledge of the size of the anion permits the estimation of the location and shape of the charge transfer to solvent band due to it.

Infrared spectroscopy and Raman spectroscopy yield evidence for ion–solvent vibrations, the frequencies and force constants of which depend appreciably on the electrical field strength of the ion, and hence on its radius on the solution. For instance, the frequencies of the symmetric stretching vibration (cation–solvent) of divalent metal ions in liquid ammonia decrease monotonously with increasing ionic radii.[15] A similar trend is observed for these frequencies in solutions of salts of the alkali-metal ions in dimethyl sulfoxide.[16] The corresponding force constants in tetrahydrofuran and dimethyl sulfoxide diminish as the ions become bigger. The presence of ions also affects the frequencies of the internal vibrations of the solvents, causing positive frequency shifts. For instance, the C—C and the C≡N vibration frequencies in acetonitrile[17] are shifted to higher frequencies, again in the order expected from the ionic radii (and charges) for the alkali metal and alkaline earth metal cations. Since for these kinds of ions the interactions between the ions and the solvents are of an electrostatic nature mainly: the nearer the solvent molecule can approach the ion, the stronger is its interaction with it, and hence this ordering of the frequencies, force constants, and frequency shifts.

III. The Radii of Ions

A. The Concept of Ionic Radii

The concept of the size of microscopic particles, such as molecules, ions, or atoms, is intuitively understood, once the notion that matter is microscopically structured is accepted. However, it is not simple to define this size precisely. The wave functions that describe the electron density around the nucleus of an isolated atom approach zero asymptotically as the distance from the nucleus increases. Hence, an isolated atom extends indefinitely into space, and some arbitrary decision (a minimal electron density still considered to "belong" to the atom) must be made about its size. For atoms in their isolated state, the van der Waals radius is an acceptable descriptor of their sizes. The collision diameters of some atoms can be measured in the gas phase by various method, and they relate well to the sums of the van der Waals radii of the colliding atoms. Molecules, being in general nonspherical, cannot simply be assigned radii, but mean radii can be assigned to them from their experimentally determined "collision diameters".

Ions are generally treated differently, since they are generally studied in condensed matter and are not usually encountered in the gas phase, i.e., in relatively isolated states where individual collisions can be noted. (This is not strictly true, since many modern techniques, ranging from mass spectrometry to ion synchrotron resonance, produce gaseous ions that can be studied.) Ions are generally found in solid crystalline ionic compounds, i.e., salts. Most of the information on the sizes of ions comes traditionally from the study of such solids, following the observation that the interionic distances $d_{\text{ion-ion}}$ in their crystals are additive in terms of the contributions of the cation and the anion. These distances are obtained with very high accuracy and precision ($\pm 0.000_3$ nm or even better) by modern X-ray diffraction techniques.

Goldschmidt[18] and Pauling[19] provided in the 1920s sets of radii for monoatomic ions, based on measured $d_{\text{ion-ion}}$ values in crystalline salts and on theoretical considerations of how these distances should be apportioned among the ions. Such radii are constant characteristics of ions in various crystal lattices, provided that the coordination number is the same as that in the crystals employed for their determination. A comprehensive list of ionic radii, valid for crystals, and mainly for coordination number 6, based on the Pauling theoretical considerations, was more recently presented by Shannon and Prewitt.[20] These radii reproduce the measured $d_{\text{cation-anion}}$ in most fluoride and oxide lattices, with the specified radii of the anions: $R(\text{F}^-) = 0.133$ nm and $R(\text{O}^{2-}) = 0.140$ nm. They are in substantial agreement with the original set of Pauling radii[19] and with their revisions by Ahrens[21] (within ±0.005 nm).

Although these Pauling-type ionic radii for coordination number 6 are widely used, they are not universally accepted, since the theoretical basis used by Pauling for the apportioning of $d_{\text{ion-ion}}$ between the cation and anion can be challenged. For instance, Gourary and Adrian[22] considered the electron density as a function of the distance from a given ion in a sodium chloride lattice. They preferred to take the extent of the space around the sodium nucleus that is to be assigned to the sodium ion as that which is limited by the minimum in the electron density curve. The Gourary and Adrian radii of cations are then considerably larger than the Pauling radii, and those of anions are considerably smaller (e.g., $R(\text{F}^-) = 0.116$ nm), since the additivity is preserved. Gourary and Adrian[22] have tabulated values of the radii of the alkali metal and the halide ions only.

The radii of polyatomic ions are more difficult to define. An operational way to their definition is via their use for the description of thermodynamic properties of salts containing such ions; see section II. Thus, thermochemical radii have been defined by Kapustinskii[23] and by Yatsimirskii[24] and have found application beyond their defining equations. A recent listing of thermochemical radii for many ions not included in the original listings of such radii was presented by Jenkins and Thakur.[25] Marcus and Loewenschuss[26] have recently suggested that for polyatomic ions of a given structure (e.g., tetrahedral oxyanions or octahedral cyano complexes) a constant ratio exists between the thermochemical radii and the characteristic intraionic distances (the distance between the nucleus of the central atom and the nuclei of the oxygen atoms or carbon atoms of the cyano groups in the above examples). For many additional ions, therefore, thermochemical radii can be assigned, if it is accepted that this constancy prevails for them, too. Such methods work best for ions that have approximate spherical symmetry, e.g., regular tetrahedral or octahedral ions, but are not expected to work well otherwise, i.e., for grossly asymmetric ions such as acetate. Ions such as nitrate or chlorate are problematic, since molecules or other ions may approach them to different proximities, depending on their direction of approach. Such ions may be assigned mean radii, with limited applicability.

It is not immediately obvious that the radii of ions that were established in crystalline compounds, whether on the basis of interionic distances $d_{\text{ion-ion}}$ or on the basis of thermochemical data, are also applicable to ions in liquid solutions. One step toward the resolution of this problem is the examination of ionic radii or $d_{\text{ion-ion}}$ values in ionic liquids, i.e., molten salts. It must be noted that due to the thermal expansion, $d_{\text{ion-ion}}$ is temperature dependent in both the crystals and melts. Experimental values of $d_{\text{ion-ion}}$ of most of the molten alkali-metal halides near the melting point were given by Levy and Danford[27] (see also Marcus[28]). They are 1–10% shorter than in the corresponding solid salts near the melting point. However, the "coordination numbers", i.e., the number of nearest neighbors, in the melts are considerably smaller than in the crystals: they are 3.5–5.6 rather than 6. The fewer the neighbors, the shorter is on the whole the distance. (This shortening is countered by a lengthening of the distances to the next nearest neighbors, which have the same sign of the charge, and hence are repulsed.) There seems, therefore, to be a close connection between the coordination number of an ion and its size not only in crystalline solids[20] but also in liquid condensed phases, and presumably also in aqueous solutions.

The following questions then arise: Are there any experimental techniques that allow the determination of accurate distances between the centers of ions and their immediately surrounding solvent molecules in solutions? If so, are there theoretical means for the extraction of ionic radii from such measured distances? The answer to the first question is definitely: yes!, as is shown in section IV. Judgment concerning the second question is deferred till the end of this review. It is necessary first to see how ionic radii might be obtained from the experimental results and their structural interpretation.

B. The Pair Distribution and Correlation Functions

The probability of the presence of a particle (molecule, atom, ion) of a given kind i in an element of volume of a homogeneous isotropic fluid (liquid) is given by its number density, $\rho_i = N_i/V$, where N_i is the number of such particles in the total volume V of the fluid. This probability is also called the singlet distribution function of i, symbolyzed by $n_i^{(1)}$.

The conditional probability of finding a particle of kind j in an element of volume at a distance r away from a given particle i in such a fluid is correspondingly called the pair distribution function. It is symbolyzed by $n_{ij}^{(2)}(r)$, provided that the particle i exerts a spherically symmetrical force field. Otherwise $n_{ij}^{(2)}$ depends not only on r but also on the mutual orientation of the particles i and j. As r tends to increasingly large distances, the conditional probability of the presence of j in the element of volume at the distance r from the origin of coordinates becomes increasingly independent of the presence of i there, and $n_{ij}^{(2)}(r)$ tends to ρ^2 (if i and j are identical in nature). At short distances, however, of the order of up to 5 molecular diameters, particle i influences the probability of the presence of particle j, and

$$n_{ij}^{(2)}(r) = g_{ij}(r)\rho^2 \qquad (7)$$

where $g_{ij}(r)$ is called the pair correlation function. (If $i \neq j$ then $\rho_i\rho_j$ replaces ρ^2.) At large values of r, therefore, $g_{ij}(r)$ tends to unity. At very small values of r, where strong repulsion excludes the j particles from the neighborhood of the i particle, $g_{ij}(r)$ is zero. At intermediate values of r, $g_{ij}(r)$ oscillates between maxima (peaks) and minima (valleys).

The number of particles j in a spherical shell of thickness dr at a distance r from a particle i is the (differential) radial distribution function

$$\mathrm{d}n_{ij}(r, \mathrm{d}r) = \rho_j g_{ij}(r)(4\pi r^2)\,\mathrm{d}r \qquad (8)$$

The integral of this radial distribution function up to a distance r' gives the number of j particles that surround the particle i up to this distance.

Although liquids and liquid solutions are devoid of long-range order, there exists short-range order in them. The partial order persists over 3–5 molecular diameters and is expressed by the deviation of the radial distribution function from the smooth parabolic function $n_{ij}(r) = \rho_j(4\pi r^2)$ or equivalently by the deviation of the pair correlation function $g_{ij}(r)$ from unity. As the distance from a given particle increases, the order in the liquid decays and is harder and harder to discern, until complete randomness in the mutual arrangement of the particles is reached. The above-mentioned deviations at short distances are the expression of the "structure" of the liquid or the solution. This structure, expressed as the $g_{ij}(r)$ function, can be obtained from experiment or computer simulation, as detailed in section IV. It leads eventually to the interatomic distances that are the subject of this review.

In the present context we are interested in particles i that are ions and particles j that are water molecules. The r value of the first peak in the dependence of $g_{ij}(r)$ on r gives the shortest interatomic (internuclear) distance d_{ij} between the two particles i and j. The region of space around the particle i from the value of r where $g_{ij}(r)$ becomes positive just before its first peak to the value of r that corresponds to the first minimum (valley) in $g_{ij}(r)$ is called the first solvation (hydration) shell of the ion i. The number of nearest j neighbors of the particle i is given by the integral of $4\pi r^2 g_{ij}(r)$ from the lower value of r to its upper value that defines this first shell. Other definitions of this number, depending on the asymmetry of the first peak in $g_{ij}(r)$, are also possible; the differences are generally minor.

Once $d_{\text{ion-water}}$ is known from the pair correlation function $g_{\text{ion-water}}(r)$, the radius of the ion, R_{ion}, can be defined as

$$R_{\text{ion}} = d_{\text{ion-water}} - R_{\text{water}} \qquad (9)$$

where R_{water} is an appropriate distance that characterizes the "radius" of a water molecule.

One approximation of this distance is half of the mean intermolecular distance $d_{\text{water-water}}$ in liquid water, that may be taken as the mean "diameter" of the water molecules. Several authors have determined the radial distribution function of liquid water, using X-ray, electron, and neutron diffraction and Monte Carlo and molecular dynamics computer simulation methods.[29-32] The resulting value of R_{water} is temperature dependent; at room temperature, where most of the determinations of $d_{\text{ion-water}}$ have been made, the average of the reported values is $R_{\text{water}} = 0.142_0 \pm 0.000_5$ nm. It can, however, be argued that the water molecules near an ion are packed closer than they are in liquid water at room temperature. If the intermolecular distance between the water molecules in ice at the melting point is taken to be a better estimate, the result is $R_{\text{water}} = 0.138_3 \pm 0.000_2$ nm.[33] This point is commented on further in section V.C.

IV. Methods for the Determination of Interparticle Distances

A. Diffraction Methods

When a monochromatic beam of radiation hits a liquid sample, some of it is transmitted unchanged, some is absorbed, but also some is diffracted at various angles θ from the direction of the incident beam. The intensities that are diffracted (scattered) at various angles provide information on the structure of the liquid. The radiation employed can be X-rays, neutrons, or electrons, and various methods revolve around the use of these kinds of radiation. Diffraction studies of the structure of liquids were reviewed in *Chemical Reviews* long ago by Kruh.[34]

1. X-ray Diffraction

In an X-ray diffraction experiment conducted on a liquid, the direct experimentally observed quantity is the intensity $I'(\theta)$ of X-rays scattered at an angle θ from the incident beam. The X-rays scattered at this angle are assigned a wavenumber k

$$k = 4\pi\lambda^{-1} \sin{(\theta/2)} \qquad (10)$$

where λ is the wavelength of the (monochromatic)

X-rays. The mean intensity of X-rays scattered from a liquid sample over a unit spatial angle, $dI/d\Omega$, is given by

$$dI/d\Omega = [I'(\theta)/a(\theta)] - \delta(\theta) \quad (11)$$

where $a(\theta)$ and $\delta(\theta)$ are calibration parameters, which have to be determined experimentally or estimated theoretically. The former depends on the sample geometry, the apparatus geometry, and the absorption in the sample and involves polarization corrections. The latter involves Compton and multiple scattering from the sample. On the other hand, the mean intensity over a unit angle is related to the properties of the liquid by

$$dI/d\Omega = N[\sum_i c_i f_i^2(k) + F_T(k)] \quad (12)$$

where N is the number of scattering centers (atoms) in the sample, c_i is the molar concentration (moles per unit volume) of the centers (atoms) of type i, and $f_i(k)$ is their coherent scattering amplitude, an inherent property that depends on k, the wavenumber of the X-ray radiation, and is available in tables. The term that is sensitive to the structure of the liquid (solution) is $F_T(k)$.

The experimentally obtained $F_T(k)$ is related to the structure by

$$F_T(k) = \sum_i \sum_j c_i c_j f_i f_j (S_{ij}(k) - 1) \quad (13)$$

where the summation extends overall the kinds of scattering atoms in the liquid sample (including the cases of $j = i$) and where the $S_{ij}(k)$ are the partial structure factors pertaining to the pairs of atoms i and j in the solution. These, in turn, are related to their pair correlation functions, $g_{ij}(r)$, as follows:

$$S_{ij}(k) = 1 + (4\pi N/kV) \int_0^\infty g_{ij}(r) \sin(kr) r \, dr \quad (14)$$

where V is the volume that contains the N scattering centers and r is a vector from particle i. A Fourier transformation can be applied to the partial structure factor, $S_{ij}(k)$, in order to obtain the individual pair correlation function $g_{ij}(r)$:

$$g_{ij}(r) = 1 + (2\pi^2(N/V)r)^{-1} \int_0^\infty (S_{ij}(k) - 1) k \sin(kr) \, dk \quad (15)$$

However, application of the Fourier transform to the experimental $F_T(k)$ data results in an observed overall $G(r)$ curve, in which the individual $g_{ij}(r)$ curves are superimposed. The individual $g_{ij}(r)$ curves must then be disentangled from the observed $G(r)$.

Several difficulties are inherent in the use of X-ray scattering from electrolyte solutions for the purpose of the determination of $g_{\text{ion-water}}(r)$ and the ion–water distance. One difficulty is the dependence of the f values, the scattering amplitudes of atoms, on k, and, in turn, on θ; see eq 10. A consequence of the k dependence of f is that the overall pair correlation function $G(r)$, which is defined by

$$G(r) = (2\pi^2(N/V)r)^{-1} \int_0^\infty F_T(k) k \sin(kr) \, dk \quad (16)$$

and results from the Fourier transform, is not a linear combination of the individual $g_{ij}(r)$ functions. Another difficulty is the insensitivity of f to light elements and, in particular, to hydrogen, so that the conformation of the water molecules near the ion cannot be determined. A further difficulty is the appearance of spurious small peaks in the Fourier-transform-calculated function $G_{ij}(r)$ at low values of r that arise from the truncation of the $S_{ij}(k)$ function at high values of k. Generally, these spurious peaks are disregarded, since the main (first large) peak stands out sufficiently clearly.

The main difficulty with the X-ray diffraction method for the determination of the ion–water interparticle distance arises from eq 13. Since the solution contains both cations C and anions A, there are six distances that contribute their partial structure factors to F_T: W–W, C–W, C–C, C–A, A–W, and A–A, where W symbolizes the oxygen atom of the water molecules nearest to the ion. This is the least number of relevant distances that applies in solutions containing only monoatomic ions and is a result of the insensitivity of the X-ray scattering intensities to the positions of the hydrogen atoms (these would have added four additional distances, W–H, H–H, C–H, and A–H).

It is in general impossible to extract the above-mentioned six distances individually from the X-ray scattering results on a solution of CA in water. This is due to the impossibility, in the case of X-ray diffraction experiments on solutions, to vary $f(k)$ of the atoms of interest in a systematic manner. An approximation to such a systematic variation is the use of isomorphous substitution. The atom of interest is substituted by another one having similar properties (with the expectation that it will have the same $g_{\text{ion-water}}(r)$ and $d_{\text{ion-water}}$) with the exception of having a different $f(k)$. This property depends strongly and monotonously on the atomic number Z of the scattering atom. This method has only seldom been applied. Recourse is generally made instead to the following procedure.

Even in the more concentrated solutions studied (e.g., those containing up to 3 mol dm^{-3} of CA in water) most of the scattered X-ray intensity still generally arises from the W–W distances, since the water molecules outnumber the ions by about 10 to 1 or more. In the often utilized first-neighbor model (FNM), the W–W distances in the bulk of the water, outside the first hydration shells of the ions, are assumed to be the same in the electrolyte solution as in pure water. Their contribution to the observed $G(r)$ may therefore be subtracted out. The interionic C–C, C–A, and A–A distances can be neglected in not too concentrated solutions, since their contribution to F_T depends on the square of the concentration. (Sometimes, however, C–A distances are important when ion pairs are formed in the solution.)

There remain, therefore, only two distances that have to be determined, C–W and A–W, provided that the FNM is applicable. The superposition of the $g_{\text{CW}}(r)$ and $g_{\text{AW}}(r)$ curves (after subtraction of the concentration-weighted $g_{\text{WW}}(r)$ curve from the "observed" $G(r)$) leads to a remaining $g(r)$ curve that exhibits the peaks at the characteristic distances C–W and A–W. These can generally be distinguished, although a second peak in the $g_{\text{CW}}(r)$ curve, due to second-nearest-neighbor water molecules of the cation C that are ignored in the FNM, may obscure the first peak in the $g_{\text{AW}}(r)$ curve in the combined $g(r)$. It is also helpful to assume a geometry and a coordination number around the ions, since then W–W distances within the first coordination shell around an ion, which would superimpose their contribution to $g(r)$ on those of the other characteristic distances, are uniquely determined by the ion–W distance. These W–W distances can be identified in the curve, and their contribution to $g(r)$ can be subtracted out.

In many cases, however, it was found that the FNM cannot account adequately for the experimental results. A second hydration shell, attached by hydrogen bonds to the first one and held also by the intense electrical field of a small and highly charged ($z > 2$) cation, must be taken into account. One consequence of this second-neighbor model (SNM) is that the amount of water present as "bulk water" is diminished. More assumptions, interatomic distances, and geometries are thus introduced by the SNM, until the desired fit of the computed F_T and the experimental one is accomplished. The price to pay for this better fit is a reduction in the credibility of the results, due to the added fitting parameters and assumptions.

In spite of all these difficulties, the ion–W distances can nowadays be determined with modern instrumentation and computation methods to a remarkable degree of accuracy in the simpler cases. Uncertainties of 0.000_3 nm are often given for the reported distances. This uncertainty may be realistic for cations, provided that the assumed geometry of the water molecules around the cation is correct, which seems to be the case for the regular octahedral first coordination shell of transition-metal ions, provided no inner-sphere complexing takes place. In other cases, a more realistic estimate of the uncertainty of the determination of the ion–W distance would be 0.001 nm or worse. In the earlier determinations, up to the late 1950s, the state of the art allowed only determinations to within 0.005 nm or worse.

2. *Neutron Diffraction*

Neutron diffraction from electrolyte solutions is applicable for the determination of the interatomic distances similarly to X-ray diffraction. Whereas X-rays are scattered by the electronic shells of the atoms, neutrons are scattered by their nuclei. The overall approximate spherical symmetry of the electronic shells cause also the X-ray diffraction results to give the relative positions of the nuclei of the atoms, so that there is no net difference between the methods arising from this respect. Equations 10–16 continue to be valid (the wavelength of the neutrons in eq 10 is obtained from their kinetic energy), but there are some very important differences. One difference arises from the factors that affect the calibration parameters $a(\theta)$ and $\delta(\theta)$. The former depends, as in X-ray scattering, on the sample and instrumental geometries and absorption by the sample, but it also depends on absorption by the sample container. The latter depends, as in X-ray diffraction, on multiple scattering, but it also depends on scattering by the container, incoherent scattering, and inelastic (Placzek) scattering. All these effects must be corrected for, either experimentally or from theoretical calculations. The Placzek corrections are, unfortunately, not fully understood and not easy to apply, but contribute heavily to the observed scattering intensities.

A major difference between X-ray and neutron scattering from solutions arises from the different dependencies of the coherent scattering amplitudes f on the wavenumber k of the radiation and on the atomic mass (mass number, A) and atomic number Z of the scattering atoms. Whereas in X-ray diffraction f decreases monotonously with k, it is independent of it for neutron scattering. On the other hand, whereas the f for X-ray scattering increases monotonously with the atomic mass of the atoms, for neutron scattering it is very sensitive to the combination of their A and Z. For certain combinations (i.e., the combination of the number of protons and neutrons in the nucleus of a given isotope of an element) f is very large, while for other combinations (in another isotope of the element) it may be near zero, of even negative. Examples for this are the values (in pm) of f for ^{1}H, −0.372, and ^{2}H (deuterium), 0.667; for ^{35}Cl, 1.17, and ^{37}Cl, 0.29; or for ^{58}Ni, 1.44, and ^{62}Ni, −0.87. A consequence of the appreciable value of f for hydrogen atoms is the sensitivity of the neutron diffraction results to the relative positions of the hydrogen atoms in the aqueous solution (so that the four distances H–H, O–H, C–H, and A–H now contribute to F_T). Therefore the average configuration of the water molecules near the ions can, in principle, be studied by the neutron diffraction method. Since ^{1}H nuclei have an appreciable absorption cross section for thermal neutrons, most scattering experiments on aqueous solutions are conducted with heavy water, D_2O, but it is assumed that this does not affect the ion–water distances or the configuration of the water molecules around the ions.

The necessity to disentangle 10 partial structure factors $S_{ij}(k)$ from the experimental F_T according to eq 13 (or 10 individual $g_{ij}(r)$ from $G(r)$ according to eq 16) makes the direct neutron diffraction method impractical—this in spite of the fact that $G(r)$ is a linear combination of the $g_{ij}(r)$, due to the independence of f for neutron scattering from k, contrary to the case of X-ray scattering. A further important complication is the uncertainty due to the large and not fully known Placzek corrections for inelastic neutron scattering.

However, a further consequence of the sensitivity of the scattering amplitude f on the isotopic composition is the possibility of using the first-order difference neutron scattering (FODNS) functions to obtain ion–water coordination values (Soper et al.,[35] Enderby and Neilson[36]). Suppose that neutron diffraction experiments are conducted on two solutions of an electrolyte CA in (heavy) water that are identical in all respects, except in the isotopic composition of, say, the cation C. Suppose also that the coherent scattering lengths of the two compositions, f_C and f'_C, differ appreciably. Then the difference between the corrected neutron scattering cross sections (intensities) between the two experiments will depend only on those terms in eq 12 that involve the cations:

$$\Delta c(k) = A_O(S_{CO}(k) - 1) + A_D(S_{CD}(k) - 1) + A_C(S_{CC}(k) - 1) + A_A(S_{CA}(k) - 1) \quad (17)$$

Here the species j in the partial structure factor S_{Cj} is O, D (for deuterium), the cation C, or the anion A, and the A_j coefficients are products of the concentrations of C and of j, the difference $f_C - f'_C$ of the two isotopic compositions of C, and f_j. Note that the water–water correlations, which dominate in the X-ray diffraction equation, are absent from eq 17. Furthermore, the terms in A_C and A_A, depending on the square of the concentration, are generally quite small compared with those in A_O and A_D, which depend on its first power, except in extremely concentrated solutions. Thus the analogous equation to (9) where $\Delta c(k)$ replaces F_T now becomes a simple linear combination of $g_{CO}(r)$ and $g_{CD}(r)$. If suitable isotopes exist for the anion, a similar pair of experiments can be conducted on solution where different isotopic compositions of the anions are employed. A further advantage of the FODNS method is the cancellation of the major part of the Paczek corrections for inelastic scattering in the difference. This reduces the uncertainty caused by them very considerably. Similarly to the FODNS method, second-order difference measurements that involve four isotopic compositions with sufficiently different f values can give information on ion–ion distances, geometries, and interactions, but this subject is outside the scope of this review.

Neutron diffraction results by the FODNS method are limited to ions from elements that have suitable pairs of isotopes, differing considerably in their neutron scattering cross sections. The results are rarely reported to better than ±0.001 nm (a study of aqueous dysprosium chloride (Annis et al.[37]) did report the Dy–O distance to $\pm 0.000_3$ nm). Contrary to X-ray diffraction results, however, those from the FODNS method are devoid of assumptions concerning the geometry of the arrangement of the water molecules around the ion.

3. *EXAFS Measurements*

Extended X-ray absorption fine structure (EXAFS) has only recently started to be employed for the determination of ion–water distances in solutions, but it has proved to be a useful tool for probing the liquid structure near the ions. It is not capable, however, of providing information on long-range order, but this is not a limitation in the present context. EXAFS shares with the differential neutron scattering method (FODNS) the capability of giving direct information on the distances involving a given atomic species (say, the cation C), contrary to the X-ray diffraction method. EXAFS does so by the choice of the absorption edge of the X-rays that are employed and the element that provides these X-rays. The primary information of the EXAFS method is $\chi(k)$ data, where χ is the absorbance of the X-rays after pre-edge subtraction and the application of appropriate corrections. Fourier transformation of the $\chi(k)$ data is then made, leading to a combined pair correlation function $G(r)$. This must be deconvoluted into the partial $g_{ij}(r)$ that constitute it, as in the differential neutron scattering method. One advantage of the EXAFS method is that it is applicable to much lower concentrations (<0.1 mol dm^{-3}) than ordinary X-ray diffraction (Licheri et al.[38]). It is therefore freer from complications due to ion pairs and the imposition of cation–anion distances on the desired cation–water and anion–water distances.

The reported uncertainties of the ion–water internuclear distances obtained by EXAFS are <0.003 nm, but these distances are generally and systematically 1–2% shorter than those obtained from X-ray or neutron diffraction. This observation, which resulted from a consideration of the entire body of data in the present review, has not been commented on so far. On the other hand, the application of EXAFS is still so recent and the amount of information gathered by it is still so scant that no great weight can as yet be placed on these results. A deterrent to a wider application of this method is the necessity of employing very intense X-ray beams, available in only a few cyclosynchrotron machines throughout the world.

4. *Other Diffraction Methods*

Electron diffraction has been applied only very rarely to the study of solutions, and aqueous electrolyte solutions in particular. In one such study of aqueous zinc bromide (Kalman et al.[39]), 68-keV (λ = 0.005 nm) electrons were employed. Corrections for scattering by the apparatus and its geometry were applied, as were corrections for atomic self-scattering, multiple scattering, and inelastic scattering. The results were in good agreement with a parallel X-ray diffraction study. No particular advantage of using electron diffraction was cited.

B. Computer Simulation Methods

Simulation by computers is a powerful method for the "experimental" generation of fluids that yields at the same time many of their properties, such as thermodynamic or transport properties, as well as their structure, in terms of the pair correlation functions. The "experimental" generation of the fluid requires as input specification the number of particles of each kind in the system, the volume of the system, the temperature or total energy of the system, the boundary conditions (generally a periodic boundary condition), and the forces that act between the particles. In general use are the molecular dynamics method, which yields not only the equilibrium structure of the fluid but also its dynamic behavior, and the Monte Carlo method, which yields the structure and equilibrium properties only.

The success of a computer simulation depends very strongly on how realistic indeed are the interparticle forces that are used. If a range of thermodynamic (or transport) properties are predicted satisfactorily, then it is probable that the structure predicted is also acceptable. With present-day computers a simulation involving 25–500 particles that yields acceptable results is possible at costs in computer time that are within the capabilities of many institutions. This capability is probably going to become more widespread in the future. The application of computer simulation methods to the study of the structure of aqueous electrolyte solutions was reviewed recently by Heinzinger.[40]

1. *The Molecular Dynamics Method*

In the molecular dynamics method one ion (or, in some cases, a cation and an anion) and a much larger number of water molecules (25 to typically 215) are placed inside a confined space of a size commonly determined by the macroscopic density of water or an electrolyte solution of the given concentration at the given temperature. They are placed there at a random configuration, and each is given a random velocity (in a random direction) at the start. The interparticle (ion–water and water–water) forces are then "switched on", and the dynamics of the system are followed as a function of time. The positions and the momenta of all the particles are determined after each small increment of time, Δt, by the application of the classical Newtonian laws of motion and the conservation of the sum of the kinetic energies of all the particles and the potential energies between each particle and its neighbors (over their effective range). After a few thousands of time intervals Δt the system reaches dynamic equilibrium, due to momentum and energy interchanges on collisions or near approaches of pairs of particles. Accumulation of the positional configurations for a few more thousands of intervals then presents a good statistical sample, which may be averaged in terms of the individual pair correlation functions, and in particular in terms of $g_{\text{ion-water}}(r)$.

In the past, when fast and highly powerful computers were not yet available, the molecular dynamics method was applied mainly to systems with very simple interparticle forces: hard disks (in two dimensions) and hard spheres (in three dimensions). In recent years the capabilities of the computers increased so much that this limitation is no longer relevant, and more or less realistic interparticle forces can be employed.

A commonly used model for the water molecules is the ST2 model,[32b] which pictures the water molecule has having a tetrahedral geometry, with the oxygen atom in the center. The angles are the regular tetrahedral ones, and there are hydrogen atoms at two of the apexes at a distance of 0.1000 nm from the center, each carrying a charge of $q = +0.23$ elementary charges. At the other two apexes there are negative charges of $q = -0.23$ elementary charges (representing the lone pairs of electrons of the oxygen atom) at distances of 0.0800 nm from the center. This charge distribution, obtained from quantum chemical calculations, is assumed, although the resultant dipole moment is somewhat higher than that measured on gaseous water molecules. The lengths of the O–H bonds and the angle between them are near those measured by electron diffraction for an isolated water molecule, but not exactly the same.

A Lennard-Jones type potential is centered on the oxygen atom to account for dispersion forces and repulsion at short distances. The Lennard-Jones potentials for both the water–water and the ion–water interactions are of the form

$$U_{ij}^{\mathrm{LJ}} = 4\epsilon_{ij}[(\sigma_{ij}/r)^{12} - (\sigma_{ij}/r)^{6}] \tag{18}$$

where ϵ_{ij} is the depth and σ_{ij} is the effective width of the potential well. The Coulombic terms for the water–water interaction are

$$U_{\mathrm{WW}}^{\mathrm{C}}(r,d) = S_{\mathrm{WW}}(r)q^{2}\sum_{i,j=1}^{4}(-1)^{i+j}/d_{ij} \tag{19}$$

where r and d are distances between oxygen centers and point charges, respectively, and $S_{\mathrm{WW}}(r)$ is a "switching function" introduced[32b] to reduce excessive, unrealistic Coulombic forces. According to this model the hydrogen bonds formed in liquid water are linear, and the intermolecular distances agree with the experimental ones measured on pure liquid water.[32]

The ions are commonly described as spheres with point charges at their centers that undergo Lennard-Jones type interactions in addition to charge–dipole interactions with the neighboring water molecules. The Lennard-Jones potential for ion–water interactions is given by eq 18, and the appropriate parameters (width and depth of the potential well) are taken from models. For cations, these are the isoelectronic noble gases, and a Berthelot-type mixing rule is adopted to obtain the ion–water interactions from the water–water and ion–ion ones. This mixing rule specifies the arithmetic mean for σ_{ij} and the geometric mean for ϵ_{ij}. Other combination rules (e.g., those of Kong[41]) have also been used. Otherwise, ab initio calculations have also been employed. The Coulombic ion–water interactions are added to the Lennard-Jones ones:

$$U_{\text{ion-W}}^{\mathrm{C}}(r,d) = -qz\sum_{i=1}^{4}(-1)^{i}/d_{i} \tag{20}$$

where z is the charge number of the ion.

It must be emphasized that the ST2 model for water and the Lennard-Jones plus ion charge–assigned water charge (q in the ST2 model) interactions for the ions are not the only ones that have been investigated or necessarily the best ones to use. The results from the molecular dynamics simulation are fairly sensitive to the input data and functional form of the interparticle forces employed, so that refinements are possible when more sophisticated models are used. Adjustments can, in principle, be applied in order to fit as well as possible the thermodynamic and transport (e.g., diffusion) properties of the system, without trying to fit explicitly the interparticle distances found by diffraction measurements. Under such circumstances the results from the molecular dynamics simulation could be taken as independent measures of the ion–water distances. It must be remembered, however, that the potential for the ion–water interactions involves a distance parameter (say, the effective width of the Lennard-Jones potential well) taken from a model, so that it may be questioned if an altogether independent estimate of the prevailing ion–water distance can be obtained from the resulting $g_{\text{ion-water}}(r)$ curve.

2. The Monte Carlo Method

The Monte Carlo method of computer simulation of fluids is similar to the molecular dynamics method in that an ion (or a pair of a cation and anion) and many water molecules (25 up to 512) are placed into a confined space with a periodic boundary at some random configuration. The density and total energy (corresponding to a given temperature) are specified, and hence also the volume of the system. The potential energy of the system is computed on the basis of assumed (normally pairwise) interactions between all the particles, employing specified interparticle forces. In each following step one particle selected at random is moved (and reoriented, if not spherical) randomly to yield a new configuration, and the new potential energy of the system is computed. If this energy is lower than the previous one, then this step is accepted and the next step is attempted. If the new potential energy is higher than the previous one, the new configuration may still be accepted, depending on how much this energy is higher, but otherwise the step is disregarded. In this manner the potential energy on the whole diminishes in successive steps, approaching equilibrium asymptotically. When equilibrium is practically achieved in the system, the potential energy fluctuates around its

TABLE I. Li–O Internuclear Distances in Aqueous Solutions

salt	W/salt	$d_{\text{ion-W}}$/nm	n	method	ref
Li^+	64	0.204	6.0	MD	47
LiCl	3–8	0.195–0.225	4	X	49[a]
LiCl	4.4–24.5	0.21		X	50
LiI	25	0.213	6.1	MD	51
Li^+	215	0.210	6.0	MC	51
Li^+	64–125	0.198	5.3	MD	52
Li^+	215	0.213	6	MD	53
LiCl	4.0	0.200		MD	54[b]
LiI	25	0.212	6.1	MD	55
LiI	25	0.2157	6	MD	56
LiI	25	0.210	6	X	57[a]
LiCl + $CoCl_2$	7.5	0.203		X	58
LiCl + $CoCl_2$	8–17	0.199–0.207	4	X	59[a]
Li^+	215	0.210	6	MC	60
Li^+	64	0.19		MC	61
LiCl	4.0	0.211, 0.221		MD, X	62
LiCl	4.0	0.218, 0.222	4	X, MD	63
LiCl	5.6–15.6	0.195	5.3–3.3	N	64
LiCl	13.9–27.8	0.208–0.217	4	X	65
LiCl	54.3	0.190	4	X	66
LiBr	8.4–25.0	0.216–0.225	4	X	67
LiI	25	0.206	7	MD	68
LiI	25	0.213	6.1	MD	69
Li^+	10	0.19–0.20	4	theory	70
Li^+	200	0.195	4.0	MC	71

[a] Assumed n. [b] The Li^+ and Cl^- ions interact.

TABLE II. Na–O Internuclear Distances in Aqueous Solutions

salt	W/salt	$d_{\text{ion-W}}$/nm	n	method	ref
Na^+	200	0.240		MC	44
Na^+	64	0.235	6.2	MD	47
$NaClO_4$	25	0.236	6.0	MD	51
Na^+	215	0.235	6.0	MC	51
Na^+	64, 125	0.229	6.0	MD	52
Na^+	215	0.237	6	MD	53
Na^+	215	0.235	6.0	MC	60
Na^+	64	0.23		MC	61
NaCl	13.9–27.8	0.242	4	X	65
NaCl	25	0.23	7	MD	68
Na^+	10	0.23–0.24	5–6	theory	70
Na^+	200	0.233	4.3	MC	71
NaCl	54.3	0.250	8	N	72
NaCl	10.2	0.241	6	X	73
NaCl	100	0.23	7	MD	74
NaCl	25	0.23	6	MD	75
NaCl	25	0.230	6	MD	76
NaI	7	0.24	4	X	77
$NaNO_3$	6.1–9.3	0.246	6	X	78
NaCl	100	0.23	6.1	MC	79

TABLE III. K–O, Cs–O, and Ag–O Internuclear Distances in Aqueous Solutions

salt	W/salt	$d_{\text{ion-W}}$/nm	n	method	ref
K^+	200	0.265		MC	44
K^+	64	0.286	7.3	MD	47
K^+	215	0.271	6.3	MC	51
K^+	64, 125	0.276	7.5	MD	52
K^+	215	0.286	6.6	MD	53
K^+	215	0.270	6	MC	60
K^+	64	0.28		MC	61
KCl	13.9, 27.8	0.280	6	X	65
K^+	10	0.285	5–7	theory	70
K^+	200	0.283	5.1	MC	71
KCl	53.7	0.270	8	N	72
KOH	3.2	0.292		X	80[a]
KCl	12.5	0.26		N	81
KF	13.3–27	0.295		X	82
KCl		0.27		X	83
CsF	25	0.322	7.9	MD	51
CsCl	13.9, 27.8	0.315	6, 8	X	65
CsF	25	0.310	7	MD	68
CsF	25	0.322	7.9	MD	84
CsCl	53.1	0.295	8	N	85
CsCl	11.1–22.2	0.315		X	86
CsF	2.3–8.0	0.313	6	X	87
$AgClO_4$	10.4	0.2410	2.0	X	88
$AgNO_3$	14.2	0.2450	2.45	X	88
$AgClO_4$	10.6	0.241	3.9	N	89[b]
$AgClO_4$	5–16.8	0.236–0.231	3–4	EXAFS	90
$AgClO_4$	3.3–16.3	0.243–0.238	4	X	91[c]
$AgNO_3$	4.3–16.6	0.243–0.242	4	X	91[c]

[a] W–W and OH^-–W distances overlap the K^+–W ones. [b] Solution contained $HClO_4$. [c] Assumed n.

TABLE IV. $O(H_3)$–O and $N(H_4)$–O Internuclear Distances in Aqueous Solutions

salt	W/salt	$d_{\text{ion-W}}$/nm	n	method	ref
HCl	3–31	0.252	4	N	44
HCl	4–96	0.252	4	X	44
DCl, DBr	54.9, 51.7	0.288	4	N	92[a]
H_2SO_4	30.5	0.275	4	X	93[b]
$HClO_4$	38.5	0.276	4	X	94[b]
HCl	4.5	0.244	3	X	95
		0.290	1		
$HClO_4$		0.275		X	96
NH_4Cl	25	0.305	8.1	MD	85
ND_4Cl	10.0	≥ 0.260	≤ 10	N	97[c]

[a] Also $n = 3$ is compatible with data. [b] Assumed n. [c] Coordination of D_2O is not well defined.

equilibrium value. The positions of all the particles are then noted and averaged over several thousand additional configurations to yield the desired pair correlation function $g_{\text{ion-water}}(r)$.

The same kinds of interparticle forces and models for the ions and the water molecules as are used for the molecular dynamics calculations can be used also for the Monte Carlo ones. However, in the applications to the present problem ab initio calculations have been used more often, with a Hartree–Fock type calculation with superimposed dispersion forces. About 10^5 configurations were collected in a typical calculation, but problems due to a possible inadequacy of the periodic boundary condition for the long-range ion–water interaction and a dependence on the number of particles included in the system may not have been solved completely satisfactorily. Again, thermodynamic quantities are obtained from the calculation (but not dynamic properties of the system), besides the structural information. The validity of the latter can be judged from the agreement of the computed thermodynamic quantities with experimentally determined ones.

The Monte Carlo method has been applied less frequently than the molecular dynamics computer simulation method for the purpose of the determination of the structure of aqueous electrolyte solutions, specifically yielding ion–water distances. Both methods have so far been confined to the study of solutions of the alkali-metal cations and halide anions, except for one study concerning the methylammonium and methylcarboxylate (i.e., acetate) ions by the Monte Carlo method.[42]

V. Ionic Radii of Individual Ions

In Tables I–XII are presented the values of the internuclear distances $d_{\text{ion-water}}$ (cf. eq 9) that have been obtained by the methods outlined in section IV and reported in the open literature till the end of 1986. The tables are arranged according to groups of ions and

TABLE V. Mg–O, Ca–O, Sr–O, and Ba–O Internuclear Distances in Aqueous Solutions

salt	W/salt	$d_{\text{ion-W}}$/nm	*n*	method	ref
Mg(II)		0.2066		X	98
$Mg(H_2PO_4)_2$	34.0	0.211	6	X	99[a]
$MgCl_2$	50	0.200	6	MD	100
$MgCl_2$	50	0.212		X	101
$MgSO_4$	20.5	0.2094	6	X	102[a]
$Mg(CH_3CO_2)_2$		0.2094	6	X	103[a]
$MgCl_2$	27.1–55.5	0.211	6	X	104
$Mg(NO_3)_2$	10.8–24.8	0.211	6	X	105
$MgCl_2$	9.8–13.0	0.21	8.1–7.9	X	106
$Mg(BF_4)_2$	14–37	0.215	6.4–6.2	X	107
$MgCl_2$	25	0.2	6	X	108
$MgCl_2$	25	0.2044		X	109
$CaCl_2$	11.1–50.0	0.239–0.246		N	46[b]
Ca(II)		0.2330		X	98
$CaCl_2$	10.6, 17.0	0.24	8.0, 8.2	X	106
$CaCl_2$	25	0.2428		X	109
$CaCl_2$	50	0.239	9.2, 6.9	MD, X	110
$CaCl_2$	12.3–55.8	0.241–0.242	6	X	111
$CaCl_2$	12.4	0.242	5.5	N	112
$CaBr_2$	26.0–44.1	0.244–0.240	6	X	113
$SrCl_2$	21.5	0.26	7.9	X	106
$SrCl_2$	26.5–34.6	0.264	8	X	114[a]
$BaCl_2$	36	0.29	9.5	X	106

[a] Assumed *n*. [b] $d_{\text{ion-W}}$ is not monotonous with the concentration.

contain the following information. Under the heading "salt" is given the salt upon solutions of which the diffraction measurements or the ion upon which the computer simulation studies have been made. The column "W/salt" presents the number of water molecules per unit formula of salt (or individual ion) present in the solution, or the range of such numbers. The value (or the range of values) of $d_{\text{ion-water}}$ in nanometers is given in the next column, as found for the first peak in the pair correlation function $g_{\text{ion-water}}(r)$. Under the heading *n* is given the coordination number found for the same peak, or assumed for it (mainly in the case of X-ray diffraction measurements). The next column gives the method employed: X is X-ray diffraction, N is neutron diffraction, MD is molecular dynamics, and MC is Monte Carlo computer simulation, while the other entries are self-explanatory. Some specific comments for individual determinations are given at the end of each table. General comments for each ion are given in the following.

A. Cations

1. Univalent Cations

Lithium. A large number of studies have been devoted to the structure of lithium salts in aqueous solutions, unfortunately with conflicting results. A group of these studies lead to Li–O internuclear distances of 0.19 nm and nearest-neighbor numbers of around 4, and the other leads to distances of 0.21 nm and around 6 nearest neighbors. This grouping is independent of the method used to arrive at the results, but it is not completely independent of the ratio of water molecules to ions in the solution. A partly systematic dependence can be discerned in Figure 1, where the distance (and the number of nearest neighbors) seems to shrink as this ratio becomes smaller. The data are collected in Table I. If the values for water/salt ratios >10 are given unit weight, those for ratios <10 are given half weight, and values reported to only two significant figures are given a weight of 0.2, then the weighted average of the internuclear distances is 0.208 nm, with a standard deviation from the mean of ±0.006 nm. This value should be applicable to dilute aqueous solutions of lithium salts.

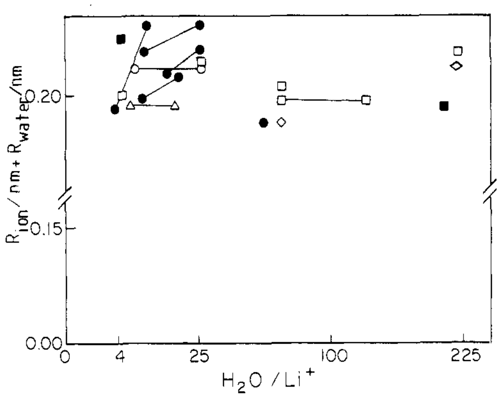

Figure 1. Li–O internuclear distance, $d_{\text{ion-water}}$ (in nm), as a function of the ratio of water molecules to Li^+ ions in solution. Empty symbols, coordination number 6; filled symbols, coordination number 4; circles, X-ray diffraction; triangles, neutron diffraction; squares, molecular dynamics simulation; diamonds, Monte Carlo simulations.

Sodium. The internuclear distances Na–O have also been determined in many studies, by both simulation and diffraction methods, and a consistent value of $0.235_6 \pm 0.006_0$ nm has been found; see Table II. The number of nearest neighbors is 6 in most of these studies, although larger values (7 or 8) and a smaller one (4) have also been employed in the interpretation of the data. No effect of the salt concentration on the distance can be discerned in the data.

Potassium. The internuclear distances K–O have been determined in several studies, mainly by simulation methods but also by diffraction methods. A consistent value of $0.279_8 \pm 0.008_1$ nm has been found; see Table III. The number of nearest neighbors employed in the interpretation of the data is between 6 and 8. No effect of the salt concentration on the distance can be discerned in the data.

Rubidium. In a single study by molecular dynamics computer simulation of a system consisting of 1 Rb^+ ion and 8 water molecules, a cluster of the rubidium ion with 5 water molecules around it was found. The Rb–O distance was given as 0.15 ± 0.01 nm + the radius of a water molecule.[43]

Cesium. Computer simulations by molecular dynamics yielded Cs–O internuclear distances of 0.31–0.32 nm with 7–8 nearest neighbors, and an X-ray diffraction study yielded similar results. A neutron diffraction study, on the other hand, yielded the shorter distance of 0.295 nm (with 8 nearest neighbors). The average of the data (disregarding the short value) is $0.313_9 \pm 0.007_6$ nm; see Table III.

Silver. Diffraction methods yielded consistent results, whether the number of nearest neighbors was taken as 4, as 2, or some value in between. The Ag–O internuclear distance is $0.241_7 \pm 0.002_1$ nm; see Table III.

Thallium(I). An X-ray diffraction study of concentrated (3.5 or 10.8 mol dm^{-3}) aqueous thallium(I) formate solutions[43a] showed the Tl atoms to be com-

TABLE VI. Mn–O, Fe–O, Co–O, and Ni–O Internuclear Distances in Aqueous Solutions

salt	W/salt	$d_{\text{ion-W}}$/nm	n	method	ref
$Mn(CH_3CO_2)_2$		0.2195	6	X	103[a]
$MnSO_4$	20–100	0.22	6.0	X	115
Mn(II)	500	0.217	6	X, EXAFS	116
$MnSO_4$	13.2–26.8	0.2218–0.2195	5.25	X	117[a,b]
$Mn(NO_3)_2$	11	0.2192	5.4	X	118[a,b]
$MnSO_4$		0.2196	6	X	119[a]
$Mn(ClO_4)_2$	21.2	0.220	6	X	120
$MnCl_2$	9.7, 7.3	0.2184	4.65, 4.45	X	121[b]
$MnBr_2$	7.7, 7.15	0.2181	5.0, 4.8	X	121[b]
Fe(II)	500	0.210	6	X, EXAFS	116
$Fe(ClO_4)_2$	25.5	0.212	6	X	120
$FeBr_2$	10.2–17.8	0.2122	5.1–5.5	X	122[b]
$CoCl_2$	14.8	0.21	6	X	27
$CoCl_2$	7.5	0.2099	5.5	X	58[b,c]
$CoCl_2$	8–17	0.2091–0.2085	5.6–6.2	X	59[b,c]
$CoCl_2$		0.214	5	X	95[b]
Co(II)		0.2091		X	98
$Co(CH_3CO_2)_2$		0.2140	6	X	103[a]
Co(II)	500	0.209	6	X, EXAFS	116[a]
$Co(ClO_4)_2$	21.0	0.208	6	X	120[a]
$CoBr_2$	11.0–18.3	0.2101–0.2086	5.3–6.0	X	122[b]
$CoCl_2$	17.9	0.210	5.5	X	123[b]
$Co(ClO_4)_2$		0.209	6.5	X	124
$CoBr_2$	17	0.211	5.9	X	125
$CoSO_4$	25–100	0.215	6.15–6.32	X	126
Ni^{2+}	64	0.217	8.0	MD	47
Ni(II)		0.2065		X	98
$NiSO_4$	27.5	0.2063	6	X	102[a]
$NiCl_2$	25	0.21	6	X	108[a]
Ni(II)	500	0.206	6	X, EXAFS	116[a]
$NiSO_4$		0.2068	6	X	119[a]
$Ni(ClO_4)_2$	22.7	0.204	6	X	120[a]
$Ni(ClO_4)_2$		0.205	6	X	123[a]
$NiCl_2$	17.9	0.207	5.5	X	124[b]
$NiSO_4$	25–100	0.215	6.15–6.32	X	126
$NiBr_2$	25.5	0.2065	5.1	X	127[b]
$NiCl_2$	11.5	0.207	5.8	N	128[d]
$NiCl_2$	11.3–580	0.207–0.210	5.8–6.8	N	129
$Ni(H_2PO_4)_2$	15.2	0.203	5.25	X	130[a,b,e]
$Ni(NO_3)_2$	13–110	0.206	6.5	EXAFS	131
$NiCl_2$	12.6–27.4	0.205	6	X	132
$NiCl_2$	12.6–645	0.205–0.210	5.8–6.8	N	133[f]
$Ni(ClO_4)_2$	14.6	0.207	5.8	N	134
$NiBr_2$	11.9–24.7	0.2079–0.2066	5.65	X	135[b]
$NiBr_2$	9.6–26.5	0.204	5.4–5.7	X	136
$NiSO_4$	27	0.2059		X	137[d]
$NiCl_2$	14–18	0.207	6	EXAFS	138
$Ni(NO_3)_2$	55	0.205		EXAFS	139
$NiCl_2$	12.6	0.205	5.8	N	141

[a] Assumed n. [b] Some ligand ions present in the inner coordination sphere beside the water molecules. [c] LiCl also present in the solution. [d] No ligand ions found in the inner coordination sphere. [e] H_3PO_4 also present in the solution. [f] $d_{\text{ion-W}}$ does not vary monotonously with the concentration.

plexed by the formate (as a tetramer at the higher concentration) but not primarily hydrated. Therefore no Tl–O(water) distances can be derived from this, the only study of aqueous Tl(I).

Hydronium. According to X-ray diffraction results, the internuclear distance between the central oxygen atom of the H_3O^+ grouping and the oxygen atom of a nearest neighbor water molecule (one of assumed four) is practically the same as between the oxygen atoms of water molecules in bulk water. Neutron diffraction results, however, yield a higher as well as a lower value (Table IV). The discrepancy cannot be ascribed to the isotopic composition of the hydrogen atoms (deuterium is used in the neutron diffraction studies), but the high concentrations employed in one study,[44] solutions with down to 3 mol of water per mol of acid, could be responsible for the low value. The presence of three nearest neighbors at the very short distance of 0.244 nm and a considerably farther neighbor at 0.290 nm resulted from a recnt interpretation of X-ray diffraction data. This result would explain the discrepancies between the results of earlier work. In dilute solutions the value $0.275_5 \pm 0.001_5$ nm for the O–O distance seems to be the best estimate.

Ammonium. No agreement exists between the results of molecular dynamics computer simulation and neutron diffraction results (Table IV). The number of nearest neighbors given, 8 or <10, respectively for the two approaches, seems to be high, and the N–O internuclear distance obtained from neutron diffraction is a very low lower limit only (0.260 nm). The value from the computer simulation, on the other hand, seems to be too high. No satisfactory estimate arises from these data.

TABLE VII. Cu-O, Zn-O, Cd-O, Hg-O, and Sn-O Internuclear Distances in Aqueous Solutions

salt	W/salt	$d_{\text{ion-W}}$/nm	n	method	ref
$CuSO_4$	48, 100	0.215 eq^{a} 0.25 ax^{a}	5.2	X	115
$Cu(ClO_4)_2$	15.7	0.194 eq 0.238 ax	4 eq 2 ax	X	120
$CuCl_2$	17.9	0.195	2.8 eq	X	124^{c}
$CuCl_2$	11.6	0.205 eq 0.25 ax	2.3 eq 2 or 0^{b} ax	N	142
$Cu(NO_3)_2$	23.5–34.7	0.2002 eq 0.222 ax		X	143^{c}
$CuCl_2$	12.9	0.205	2.3 eq	N	144^{b}
$CuBr_2$	>100	0.193	7	EXAFS	145^{c}
$CuBr_2$	12–100	0.193	3.5	EXAFS	146^{c}
$CuBr_2$	10.8–53.1	0.197 eq 0.250 ax	2.5–3.7 eq 2 ax	X	147^{c}
$CuSO_4$	75, 160	0.21 eq 0.23 ax	4.1 eq 2.2 ax	X	148
$Cu(ClO_4)_2$	11.4	0.194 eq 0.243 ax	4 eq 2 ax	X	149
$CuBr_2$	>1000	0.197		EXAFS	151
$ZnBr_2$	8.1–15.9	0.221	2.4	X, EL	26^{c}
Zn(II)		0.2093		X	98
$Zn(CH_3CO_2)_2$		0.2076	6	X	103^{d}
$ZnSO_4$	31–100	0.215	6	X	115
$Zn(ClO_4)_2$	19.4	0.208	6	X	120
$ZnBr_2$	7–610	0.194	2.5–7	EXAFS	145^{c}
$ZnSO_4$	27.1	0.2107	6	X	152^{a,e}
$ZnSO_4$	18.6	0.210	6	X	153^{d}
$Zn(NO_3)_2$	9.0	0.217	6.6	X	154
$ZnCl_2$	5.4	0.205		X	155^{f}
$ZnSO_4$	25	0.2100	6	X	156^{d}
Cd(II)		0.2289		X	98
$Cd(CH_3CO_2)_2$		0.2287	6	X	103^{d}
$Cd(H_2PO_4)_2$	10.4	0.230	5.1	X	130^{d,g}
$Cd(ClO_4)_2$	23.0	0.229	6	X	157^{d,g}
$CdSO_4$	17.6	0.229	5.2	X	157^{c,d}
$CdSO_4$	25	0.231	6	X	158^{d,h}
$Cd(NO_3)_2$	9–54	0.2272	5.7	X	159
$CdCl_2$	35–63	0.237	4	X	160^{c}
$Cd(ClO_4)_2$	26.6	0.231	6	X	161^{d}
$CdBr_2$	13.2–662	0.218	3	EXAFS	162^{c}
$Hg(BF_4)_2$	27	0.233	6	X	163^{d}
$Hg(ClO_4)_2$	19.7	0.234	6	X	164^{i}
$Hg(ClO_4)_2$	19.7	0.241	6.0	X	165
$Sn(ClO_4)_2$	16.8	0.234 0.221	3.5 3.8	X EXAFS	48^{j}
$Sn(ClO_4)_2$	12.0	0.233 0.283	2.4 3.0	X	150^{k}

[a] Equatorial and axial water molecules in the Jahn–Teller distorted octahedral inner coordination sphere. [b] If $n = 0$ then there are 4 Cl^- ions in the equatorial positions. [c] Some ligand ions present in the inner coordination sphere. [d] Assumed n. [e] No ligand ions in the inner coordination sphere. [f] Tetrahedral species $ZnCl_2(H_2O)_2$. [g] H_3PO_4 or $HClO_4$ also present in the solution. [h] Data also at 9 and 62 °C. [i] Data also for hydrolyzed Hg(II). [j] Another model, with additional 3.0 H_2O at 0.29 nm also compatible with the data. [k] Both long and short distances present.

Methylammonium. A single study by Monte Carlo computer simulation, in a system with 216 water molecules and 1 $CH_3NH_3^+$ ion, led to 3.5 nearest neighbors, on the average, with a C–O internuclear distance of 0.37 nm or a (C)H–O distance of 0.185 nm.[42]

2. Divalent Cations

Beryllium. A study by Yamaguchi et al.,[45] involving both molecular dynamics computer simulation and X-ray diffraction, yielded conflicting results. The former method produced an octahedral arrangement of six water molecules in the first hydration shell of the beryllium, with a Be–O internuclear distance of 0.175 nm, as well as an indication of the presence of a second

TABLE VIII. Al-O, Y-O, Cr-O, Fe(III)-O, Rh-O, In-O, Tl(III)-O, and Th-O Internuclear Distances in Aqueous Solutions

salt	W/salt	$d_{\text{ion-W}}$/nm	n	method	ref
$AlCl_3$	23.8–54.0	0.188–0.190	6	X	166^{a}
$Al(NO_3)_3$	14.5	0.187	6	X	167^{a}
$Al(NO_3)_3$	100	0.190	6	X	168^{a}
$Y(ClO_4)_3$	12.4	0.2365	8.0	X	169^{a}
$Y(ClO_4)_3$	18–55	0.2368		X	170
Cr(III)	500	0.200	6	X, EXAFS	116
$Cr(NO_3)_3$	100	0.198	6	X	168^{a}
$CrCl_3$	23.4	0.1995	6	X	171^{a,b}
$Cr(SO_4)_{1.5}$	18.7	0.194	5.1	X	172^{a-c}
$CrCl_3$	64.8	0.199	6	X	173^{a}
$Cr(NO_3)_3$	24.5–50.8	0.200	6	X	174^{a}
$CrCl_3$	223	0.190	6	X	175^{a}
$CrCl_3$	17.9, 26.5	0.1982, 0.1971	6	X	176^{a}
Fe(III)	500	0.202	6	X, EXAFS	116
$Fe(NO_3)_3$	6.6–32.5	0.203–0.205	6	X	178
$FeCl_3$	6.7–21.5	0.205–0.208	2.7–4.2	X	179^{a,c}
$Fe(SO_4)_{1.5}$	14.4–20.0	0.2017	6	X	180^{a}
$Fe(ClO_4)$	21.3–29.7	0.2008	6	X	181^{a,b}
$FeCl_3$		0.207	4	X	182^{c}
$Rh(ClO_4)_3$	38.5	0.204	6.3	X	94^{b}
$Rh(ClO_4)_3$	278	0.2062	6	X	96
$Rh(NO_3)_3$	61, 145	0.2023		X	183^{d}
$In(SO_4)_{1.5}$	14.2	0.2156	6	X	184^{a,c}
$In(ClO_4)_3$	11.3	0.215	6	X	185
$Tl(ClO_4)_3$	17.1–42.3	0.2236	5	X	187
$Tl(ClO_4)_3$		0.2227	6	X	188
$Th(NO_3)_4$	57.0	0.255	5.5	X	189^{c}
$Th(NO_3)_4$	22.3	0.251		X	190

[a] Assumed a. [b] HCl, $HClO_4$, or H_2SO_4 also present in the solution.[c] [c] Some ligand ions also present in the inner coordination sphere. [d] Dimeric species, with OH^- and NO_3^- bridges.

TABLE IX. La–O, Ce–O, Pr–O, Nd–O, Sm–O, Eu–O, Gd–O, Tb–O, Dy–O, Er–O, Tm–O, and Lu–O Internuclear Distances in Aqueous Solutions

salt	W/salt	$d_{\text{ion-W}}$/nm	n	method	ref
$La(ClO_4)_3$	12.0	0.2570	8.0	X	169^{a}
$LaCl_3$	20.8–31.9	0.248	8.0	X	190
$LaCl_3$	14.6–27.8	0.258	9.1	X	191
$LaBr_3$	20.9	0.248	8.0	X	192
$Ce(NO_3)_3$	25.4	0.2552	7.5	X	193
$PrCl_3$	14.6	0.254	9.2	X	191
$NdCl_3$	16.5	0.251	8.9	X	191
$NdCl_3$	17.5	0.248	8.5	N	194
$NdCl_3$	17.5	0.2479	8.4	N	195
$NdCl_3$	32.1–99.1	0.241	8.0	X	196
$Sm(ClO_4)_3$	15.2	0.2455	8.0	X	169^{a}
$SmCl_3$	38.8	0.242	9.9	X	197
$SmCl_3$	17.2	0.247	8.8	X	198
$EuCl_3$	17.2	0.245	8.3	X	198
$GdCl_3$	26.8	0.240	9.9	X	197
$GdCl_3$	14.4–45.1	0.237	8.0	X	196, 199
$Tb(ClO_4)_3$	13.7	0.2400	8.0	X	169^{a}
$Tb(ClO_4)_3$	18–55	0.240		X	170
$TbCl_3$	11.0	0.241	8.2	X	200
$DyCl_3$	11.7	0.240	7.9	X	200
$DyCl_3$	21.0	0.2370	7.4	N	201^{b}
$Er(ClO_4)_3$	12.1	0.2360	8.0	X	169^{a}
$Er(ClO_4)_3$	18–55	0.236		X	170
$ErCl_3$	10.8	0.237	8.2	X	200
$ErCl_3$, ErI_3	4.6–15	0.23	6.3–6.5	X	202
$TmCl_3$	10.6	0.236	8.1	X	200
$LuCl_3$	10.6	0.234	8.0	X	200

[a] Assumed n. [b] No Cl^- in inner coordination sphere.

TABLE X. F–O, Br–O, and I–O Internuclear Distances in Aqueous Solutions

salt	W/salt	$d_{\text{ion-W}}$/nm	n	method	ref
CsF	25	0.264	6.8	MD	51
F^-	215	0.260	4.1	MC	51
F^-	64, 125	0.267	5.8	MD	52
F^-	215	0.263	5	MD	53
F^-	215	0.260	6.3	MC	60
CsF	25	0.322	8	MD	68
F^-	10	0.275	4–6	theory	70
KF	13.3, 27	0.262		X	82
CsF	25	0.264	6.8	MD	84
NH_4F	3.6	0.287	6	X	203
$ZnBr_2$	8.1–15.9	0.345	4.2	X	26
LiBr	25.0	0.329	6	X	67
LiBr	5.6–22.2	0.343–0.337	7.2–8.9	X	86
DBr	51.7	0.321	6	N	92[a]
$CaBr_2$	26.0–44.1	0.334–0.332	6	X	113
$NiBr_2$	25.5	0.312	5.15	X	127[b]
$ZnBr_2$	15–150	0.340	4	EXAFS	145
NH_4Br	7.6	0.336	6	X	203
LiI	25	0.368	8.7	MD	55
LiI	25	0.370		MD	56
LiI	25.2	0.363	6.9	X	57
LiI	25	0.30	7	MD	68
NaI	7	0.360	6	X	77
LiI	11.1–22.2	0.365–0.369	8.8–8.9	X	86
NaI	5.6	0.376		X	86
NH_4I	8.2	0.361	6	X	203

[a] Also $n = 4$ and $n = 8$ are compatible with the data. [b] Some of the Br^- is in the inner sphere of the Ni(II).

TABLE XI. Cl–O Internuclear Distances in Aqueous Solutions

salt	W/salt	$d_{\text{ion-W}}$/nm	n	method	ref
Cl^-	64	0.323	5.9	MD	47
LiCl	3–8.2	0.318–0.310	6	X	49[a]
Cl^-	64, 125	0.329	7.2	MD	52
Cl^-	215	0.348	8.5	MD	53
LiCl	4.0	0.320		MD	54[b]
$CoCl_2$ + LiCl	7.5	0.316	6	X	58[a]
$CoCl_2$ + LiCl	8–17	0.3156	6.0–6.4	X	59
Cl^-	215	0.325	8.4	MC	60
LiCl	4.0	0.322		MD	62
LiCl	4.0	0.319, 0.315		X, MD	63
LiCl	5.6–15.6	0.329–0.334	5.3–5.9	N	64
LiCl	13.9	0.308	6	X	65
NaCl, KCl	13.9–27.8	0.308–0.316	6	X	65
LiCl	54.3	0.310	6	N	66
LiCl	25	0.27	7	MD	68
Cl^-	10	0.345	6–7	theory	70
NaCl, KCl	54.3	0.310		N	72
NaCl	10.2	0.316	6	X	73
NaCl	100	0.27	8	MD	74
NaCl	25	0.32	6	MD	75
NaCl	25	0.330	8	MD	76
LiCl	8	0.324		X	80
NH_4Cl	25	0.322	8.2	MD	85
LiCl	5.6–22.2	0.315–0.320	6.2–7.3	X	86
DCl	54.9	0.310	6	N	92
$CoCl_2$		0.3120	5.06	X	95
$RhCl_3$ + HCl		0.3185		X	96
$MgCl_2$	50	0.318	7.0	MD	100
$MgCl_2$	50	0.316		X	101
$MgCl_2$	27.1–55.5	0.314	6	X	104
$MgCl_2$	25	0.3130		X	109
$CaCl_2$	50	0.319, 0.312	7.9, 8.2	MD, X	110
$CaCl_2$	12.3–55.8	0.315	6	X	111
$CaCl_2$	12.4	0.325	5.8	N	112
$SrCl_2$	26.5–34.6	0.323		X	115
$CoCl_2$	17.9	0.311	6	X	123[c]
$NiCl_2$	17.9	0.306	6	X	124
$NiCl_2$	11.5	0.320	5.7	N	127[d]
LiCl	3.4–14.0	0.334–0.325	5.9–4.4	N	129
$NiCl_2$	12.6–27.4	0.313	6	X	132
NaCl	9.4	0.320	5.5	N	141
$AlCl_3$	23.8–54.0	0.311–0.314	6	X	166
$CrCl_3$	23.4	0.3135		X	171[e]
$FeCl_3$	6.7–21.5	0.324–0.3156	6	X	179[c]
LiCl	3	0.320	4	MD	186
NH_4Cl	8.5	0.317	6	X	203
LiCl	3.4	0.325	4	N	204[b]
HCl	8–27	0.320–0.325		X	205
HCl	4–96	0.313	4	X, N	206
NaCl, RbCl	10.4	0.320	5.5	N	207
$BaCl_2$	50.4	0.326	6.2	X	207
KCl	14.9	0.316			208
$NdCl_3$	17.5	0.329	3.9	N	209[f]

[a] Assumed n. [b] Direct interaction between Li^+ and Cl^-. [c] Some of the Cl^- present in the inner coordination sphere of the metal ion. [d] None of the Cl^- is in the inner coordination sphere of the metal ion. [e] Some HCl also present. [f] Some of the water shared between the Nd^{3+} and Cl^- ions.

hydration shell, at a mean distance of 0.373 nm from the beryllium atom. The other method indicated the presence of only four water molecules in the first hydration shell, at a Be–O distance of 0.167 nm, but this at a lower number of moles of water per mole of salt (10), compared with the ratio in the former study (50). The number of water molecules near the chloride anions at the higher concentration, 3.4, was also much lower than in the more dilute solution (7), indicating the formation of contact ion pairs in the concentrated one. This could explain the smaller number of water molecules, and perhaps also the shorter distance. On the other hand, a coordination number of 6 for the beryllium in the dilute solution is surprising, 4 being the expected number. It is evident that this system merits further study before a firm conclusion can be reached.

Magnesium. The results of several studies (Table V) by X-ray diffraction are consistent. With the assumption of a nearest-neighbor number of 6, the average Mg–O internuclear distance is $0.209_0 \pm 0.004_1$ nm. A molecular dynamics computer simulation study yielded, with the same number of neighbors, the somewhat lower value of 0.200 nm.

Calcium. Calcium salt solutions have been studied by molecular dynamics computer simulation as well as by neutron and X-ray diffraction methods, with generally consistent results concerning the Ca–O internuclear distance (Table V): $0.242_2 \pm 0.005_2$ nm. However, no agreement concerning the number of nearest neighbors resulted, the reported values ranging from 5.5 to 10.0, possibly depending on the concentration (Hewish et al.[46]). A recent molecular dynamics study, however, reported a considerably larger Ca–O distance, 0.254 nm in a system with 64 water molecules per Ca^{2+} ion.[47]

Strontium. An X-ray diffraction study reported the Sr–O internuclear distance as 0.264 ± 0.004 nm with an assumed 8 nearest water molecule neighbors of the strontium ion. An earlier study reported 7.9 for the number of neighbors and estimated the internuclear distance at 0.26 nm (Table V).

Barium. An early and uncorroborated study reported 9.5 for the number of neighbors and estimated the internuclear distance at 0.29 nm (Table V).

Manganese. Several X-ray diffraction studies of manganese salt solutions yielded consistent results. In some of these studies, contact ion pairs with the anions were disregarded, and the number of nearest water neighbors was assumed to equal the coordination number of 6. In others, ion pairing was explicitly taken into

TABLE XII. $N(O_3)$-O, $Cl(O_4)$-O, $(H_2)P(O_4)$-O, $C(H_3CO_2)$-O, $S(O_4)$-O, $Se(O_4)$-O, and $Mo(O_4)$- or $W(O_4)$-O Internuclear Distances in Aqueous Solutions

salt	W/salt	$d_{\text{ion-W}}$/nm	n	method	ref
$NaNO_3$	6.1, 9.3	0.318	3 or 6	X	78
$AgNO_3$	14.2	0.317	4.3	X	88
$AgNO_3$	4.3–16.6	0.313	1	X	91
$Mn(NO_3)_2$	11	0.344	6.3	X	118[a]
$Zn(NO_3)_2$	9.0	0.344	17.7	X	154
$Cd(NO_3)_2$	11–54	0.349	8.8	X	159
$Al(NO_3)_3$	14.5	0.339		X	167
$Rh(NO_3)_3$	61.1, 144.9	0.350	8.2	X	183
$Ce(NO_3)_3$	25.4	0.340	7.0	X	193
$NaNO_3$	6.4	0.265 ax	1.3 ax	N	211
		0.340 eq	2.4 eq		
NH_4NO_3	4.1	0.351	9	X	212
$AgClO_4$	10.4	0.3570	25.6	X	88
$AgClO_4$	16.3	0.352	1	X	91
$Rh(ClO_4)_3 + HClO_4$	278	0.376	12	X	96
$Ln(ClO_4)_3$	12.0–15.2	0.380	8	X	169[b,m]
$Fe(ClO_4)_3 + HClO_4$	8.9–20.1	0.380–0.367		X	181
$NaClO_4$	17.1	0.37	4–5	N	211
$Mg(H_2PO_4)_2$	34.0	0.387	8.8	X	99[c]
$Ni(H_2PO_4)_2$	15.2	0.375	4.2	X	130[c,d]
$Cd(H_2PO_4)_2$	10.4	0.391	4.4	X	130[c,d]
PO_4^{3-}	6–18	0.306		MD	212[e]
H_3PO_4	7.7–25.0	0.360–0.373	4 or 8	X	213[a,f]
$CH_3CO_2^-$		0.37		MC	29
$Mg(CH_3CO_2)_2$		0.36–0.37	4–6	X	103[g]
$Co(CH_3CO_2)_2$		0.36–0.37	4–6	X	103[g]
$Mn(CH_3CO_2)_2$		0.36–0.37	4–6	X	103[g]
$Cd(CH_3CO_2)_2$		0.36–0.37	4–6	X	103[g]
$Zn(CH_3CO_2)_2$		0.35	4–6	X	103[g]
H_2SO_4	30.5	0.367	8	X	81[b]
$MgSO_4$	20.5	0.370	7.7	X	102
$NiSO_4$	27.5	0.381	8.1	X	102
$MnSO_4$	13.2–26.8	0.3905	7.4	X	117[h]
$MnSO_4$		0.382	8.0	X	119[h]
$NiSO_4$	18, 27	0.380	8.2	X	137[k]
$ZnSO_4$	27.1	0.387	7.0	X	152[i]
$ZnSO_4$	18.6	0.383	8.2	X	153
$ZnSO_4$	25	0.387	6.6, 7.3	X	156
$CdSO_4$	25	0.389	6.9	X	158[h,j]
$Cr(SO_4)_{1.5}$	18.7	0.381	7.8	X	172[h]
$Fe(SO_4)_{1.5}$	9.6–13.4	0.372–0.377	18–20	X	180
$In(SO_4)_{1.5}$	14.7	0.389	6.4	X	184[h]
$(NH_4)_2SO_4$	11.7	0.379	7.6	X	214
$Ln(SeO_4)_{1.5}$	24.5–46.4	0.395	8	X	169[b,c,l]
Na_2MoO_4	25	0.406	12	X	215
Na_2WO_4	25	0.406	12	X	215

[a] Some of the NO_3^- is in the inner coordination sphere of the metal ion. [b] Assumed n. [c] Some of the $H_2PO_4^-$ is in inner coordination sphere of the metal ion. [d] H_3PO_4 is also present in the solution. [e] Small cluster. [f] Two models are compatible with the data. [g] Some of the $CH_3CO_2^-$ is in the inner coordination sphere of the metal ion. [h] Some of the SO_4^{2-} is in the inner coordination sphere of the metal ion. [i] None of the SO_4^{2-} is in the inner coordination sphere of the metal ion. [j] Data also at 9 and 62 °C. [k] Data also for solutions containing added Li_2SO_4. [l] Some SeO_4^{2-} is in the inner coordination sphere of the metal ion. [m] Ln = La, Sm, Tb, Er, or Y.

account, as a result of the finding of the characteristic cation–anion distances in the solution, so that the number of water molecules was lower. Still, the Mn–O internuclear distances found in all the studies are nearly the same, $0.219_2 \pm 0.001_3$ nm, on the average; see Table VI.

Iron(II). The X-ray studies of solutions of iron(II) salts all yielded the Fe–O internuclear distance near the average of $0.211_4 \pm 0.001_0$ nm with an assumed 6 nearest neighbors of either water molecules or bromide anions and water molecules; see Table VI.

Cobalt. Several X-ray diffraction studies of cobalt salt solutions yielded consistent results. In some of these studies, contact ion pairs with the anions were disregarded, and the number of nearest water neighbors was assumed to equal the coordination number of 6. In others, ion pairing was explicitly taken into account, as a result of the finding of the characteristic cation–anion distances in the solution, so that the number of water molecules was lower. Still, the Co–O internuclear distances found in all the studies are nearly the same, $0.210_6 \pm 0.002_2$ nm, on the average; see Table VI.

Nickel. Many studies have been concerned with nickel ions in aqueous solutions, comprising X-ray and neutron diffraction and EXAFS, as well as molecular dynamics computer simulation. In the X-ray diffraction studies, the number of nearest neighbors was assumed to be 6, whether they were only water molecules or both these and anions, but the isotope-differential neutron diffraction studies produced 5.8 nearest water molecules at the highest concentrations (about 13 mol of water per mol of salt), which increased to 6.8 nearest neighbors in the more dilute solutions (near 600 mol per mol). The molecular dynamics study, however, yielded the value of 8 neighbors (in a system of 64 water molecules and 1 Ni^{2+} ion), which is excessive relative to the known coordination number of 6. In all cases, however, the Ni–O internuclear distance was near to the average of $0.206_1 \pm 0.001_4$ nm; see Table VI.

Copper(II). It is impossible to assign a unique Cu–O internuclear distance to ions of Cu^{2+} in aqueous solutions because of the Jahn–Teller distortion of its octahedral first coordination shell. There are four shorter equatorial distances and two longer axial ones. A further complication is the propensity of copper(II) ions to be complexed by halide and nitrate anions in the relatively concentrated solutions required for the diffraction studies. When the appropriate coordination numbers of 4 near and 2 far water neighbors are assumed, then X-ray diffraction of copper(II) perchlorate solutions indeed yields definite Cu–O distances. These agree well with the averages obtained for these distances to the water oxygen atoms in chloride, bromide, and nitrate solutions, notwithstanding that some of the other coordination sites are occupied by atoms from the anions. These averages are $0.196_8 \pm 0.004_7$ nm for the equatorial oxygen atoms and 0.240 ± 0.010 nm for the axial ones. The results from neutron diffraction and from EXAFS are on the high and low sides of the average of the X-ray diffraction results, but within the standard deviation; see Table VII.

Zinc. A number of X-ray diffraction studies yielded consistent values for the Zn–O internuclear distance in aqueous zinc salt solutions, where the number of nearest neighbors was assumed to be 6. In some cases (the bromide and sulfate; see Table VII) inner-sphere complexing takes place, but in the case of the sulfate this does not affect appreciably the distance to the water molecules. The average distance is $0.209_8 \pm 0.006_6$ nm. Longer and shorter Zn–O distances resulted from the interpretation of the data on zinc bromide solutions by X-ray diffraction and EXAFS, respectively, when allowance was made for the presence of bromide ions in the inner coordination shell.

Cadmium. Several X-ray diffraction studies yielded consistent values for the Cd–O internuclear distance in aqueous cadmium salt solutions, where the number of nearest neighbors was assumed to be 6. In the case of the nitrate the number of nearest water neighbors found was only 5.7, but no indication of the presence of the nitrate anion in the inner coordination shell was given. On the contrary, phosphate and sulfate ions were found in this shell in other studies (Table VII), but their presence did not affect the Cd–O distance appreciably. The average value of this distance is $0.230_1 \pm 0.002_5$ nm. Only in the case of cadmium chloride solutions is there an indication of a decrease of the number of nearest water molecules to 4, when 2 chloride anions occupy sites in the inner shell, with a concomitant increase of the Cd–O distance.

Mercury(II). Mercury(II) was one of the earliest ions for which a cation–water distance was estimated from X-ray diffraction measurements on aqueous solutions. This early value was later confirmed, but still later revised when it was realized that the relatively short distance (0.233 nm) was characteristic for hydrolyzed mercury(II) ions, rather than for the unhydrolyzed Hg^{2+} aqueous ion. For the latter, the Hg–O distance is 0.242 nm, with 6.0 ± 0.4 nearest water molecules; see Table VII.

Tin(II). A study of a 3.3 mol dm^{-3} aqueous solution of tin(II) perchlorate by X-ray diffraction and EXAFS measurements was made by Yamaguchi et al.[48] The X-ray measurements yielded 0.235 nm for the Sn–O distance with 3.5 ± 0.1 nearest water molecules, but a weaker interaction with a further (assumed) 3 water molecules at 0.29 nm was also indicated. A second coordination shell of 7.2 water molecules was found at 0.44 nm, so that the 0.29-nm distance should be ascribed to water molecules in the first coordination shell. The EXAFS study yielded a shorter distance, 0.227 nm, for 3.1 nearest water molecules and an even shorter one, 0.221 nm, for another 1.1 water molecules, for an altogether occupation of about 4 water molecules in the first coordination shell. In another study, an average of 2.4 shorter internuclear distances of 0.233 nm and another 3.0 longer distances of 0.283 nm is in agreement with the above. The weighted mean distance of 0.262 is only a rough indication of the mean distance of the water molecules from the tin(II) ion.

3. *Trivalent Cations*

Aluminum. Three X-ray diffraction studies gave consistent results (see Table VIII): with assumed 6 nearest water molecule neighbors the Al–O internuclear distance was $0.188_7 \pm 0.001_5$ nm.

Yttrium. An X-ray diffraction study (Table VIII) on perchlorate solutions yielded with an assumed 8 nearest water neighbors a Y–O internuclear distance of 0.236_5 nm. In selenate solutions this distance was apparently somewhat shorter, 0.233 nm.

Lanthanides. X-ray diffraction studies of aqueous solutions of salts of most of the lanthanides (except promethium, holmium, and ytterbium) and neutron diffraction studies of aqueous neodymium and dysprosium chlorides (Table IX) yielded M–O distances and in some cases numbers of nearest-neighbor water molecules of M, where M = La, Ce, Pr, Nd, Sm, Eu, Gd, Tb, Dy, Er, Tm, and Lu. A downward trend of the number of water molecules in the first coordination shell, along with a shrinking of the M–O distance can be discerned in Table IX, but the data are not sufficiently in agreement to indicate whether the decrease in the number of neighbors is gradual or abrupt, as has been claimed (see ref 202a).

Chromium. Several X-ray diffraction studies of various chromium(III) salt solutions gave consistent results, with an assumed number of 6 nearest water molecule neighbors, for the Cr–O internuclear distance of $0.196_9 \pm 0.003_2$ nm. An EXAFS study gave concordant results; see Table VIII.

Iron(III). Several X-ray diffraction studies of various iron(III) salt solutions gave consistent results for the Fe–O internuclear distance of $0.203_1 \pm 0.001_9$ nm, with in one case 5.8 + 0.2 and in others an assumed number of 6 nearest water molecule neighbors. An EXAFS study gave concordant results; see Table VIII. In chloride solutions some chlorine atoms occupied sites in the first coordination shell, and then the Fe–O distance was somewhat longer (Table VIII).

Rhodium(III). An X-ray diffraction study of aqueous rhodium(III) nitrate solutions showed the presence of dimeric species with OH and NO_3 bridges and Rh–O distances of 0.202_0 and 0.202_6 nm to the water molecules in the remaining sites of the first coordination shell. A similar distance, 0.204 nm, was found for the Rh–O distance with 6.3 nearest neighbors in acidified perchlorate solutions; see Table VIII.

Indium. Three X-ray diffraction studies on indium sulfate and perchlorate solutions gave consistent results of 0.215_6 and 0.215 nm for the In–O internuclear distance to the (assumed) 6 nearest water molecules, although in the sulfate case there was an indication of the presence of sulfate in the inner coordination shell; see Table VIII.

Thallium(III). Two X-ray diffraction studies of aqueous thallium(III) perchlorate solutions yielded the mean Tl–O internuclear distance $0.223_1 \pm 0.000_5$ nm with 5 ± 1 nearest-neighbor water molecules; see Table VIII.

4. Tetravalent Cations

Thorium. In two studies of aqueous thorium nitrate solutions the main interest was the structure of the hydrolyzed species, but the results for acidified solutions, where no hydrolysis took place, were also reported. According to these studies, 3.5 nitrate anions are present as bidentate ligands in the inner coordination sphere of the thorium, but 5.5 water molecules complete the inner coordination shell of about 12. The Th–O(water) internuclear distance is 0.253 nm; see Table VIII.

B. Anions

Fluoride. The internuclear distance F–O was studied practically only by computer simulation methods, and only one X-ray diffraction study was reported; see Table X. This, indeed, gave a rather high value, 0.287 nm, for this distance in a very concentrated aqueous ammonium fluoride solution. So did also one of the molecular dynamics computer simulation studies (0.322 nm, with 8 nearest neighbors in a dilute solution), but the other computer simulation studies yielded the average value of $0.263_1 \pm 0.002_5$ nm, with between 4.1 and 6.8 nearest water molecule neighbors of the fluoride anion.

Chloride. A large number of studies of aqueous metal chloride solutions by diffraction and computer simulation methods report also the Cl–O internuclear distance. A few computer simulation studies were devoted specifically to the chloride anion in aqueous solutions. Apart from a few exceptions, the reported values are within the error limits of the average $0.318_7 \pm 0.006_7$ nm, but the reported number of nearest water molecule neighbors of the chloride anion range from somewhat less than 6 to 8.5, with particularly low values (see Table XI) in very concentrated solutions, where solvent-sharing ion pairs are formed.

Bromide. The internuclear distance Br–O was studied mainly by X-ray diffraction, whereas a neutron diffraction study and an EXAFS study gave low and high values relative to the X-ray results. In the latter the number of nearest water molecule neighbors to the bromide anion was generally assumed to be 6; see Table X. The average distance obtained is $0.337_3 \pm 0.005_4$ nm, outlying values being obtained in the cases of concentrated solutions of $ZnBr_2$ and $NiBr_2$, where bromide ions are in the first coordination shells of the metal ions.

Iodide. The internuclear distance I–O in aqueous solutions was studied by both X-ray diffraction and molecular dynamics computer simulation, with generally consistent results, giving an average of $0.364_7 \pm 0.003_6$ nm, with an assumed 6 or 7 nearest water molecule neighbors in the X-ray diffraction studies and 8.7 nearest neighbors in the computer simulation. One outlying very short distance, 0.30 nm, obtained in a molecular dynamics study (see Table X) is difficult to explain.

Nitrate. The nitrate anion, like the other oxyanions, poses the difficulty of the distinction between the internal internuclear distances and the external N–O one, relevant to the anion-to-water molecule distance, and hence to the ionic radius in the solution. Furthermore, the nitrate anion is not spherically symmetrical, and differences exist between the extension of the anion in the plane of its tree oxygen atoms (the equatorial radius) and perpendicular to it (the axial radius). Still, a fairly consistent picture arises from the various X-ray diffraction studies and the single neutron diffraction study; see Table XII. The equatorial N–O(water) distance is $0.345_1 \pm 0.004_3$ nm, on the average, whereas the axial water molecule can approach the nitrogen atom to within 0.265 nm, so that the overall mean N–O(water) distance is $0.316_0 \pm 0.002_2$ nm. It is, thus, impossible to assign the nitrate anion a "fixed" radius in aqueous solutions.

Perchlorate. The perchlorate anion poses less difficulties than the nitrate anion, because it is more symmetrical, but only a few studies, involving diffraction methods, report the Cl–O(water) internuclear distance. This is larger, 0.380 nm, in aqueous solutions of trivalent metal perchlorates and smaller (down to 0.352 nm) in solutions of univalent ones or in solutions containing both iron(III) perchlorate and perchloric acid. Only an imprecise value of 0.37 ± 0.01 nm can be given as an average from these studies; see Table XII.

Phosphate. Three studies by X-ray diffraction on aqueous divalent metal dihydrogen phosphate solutions yielded values for the P–O(water) distance ranging from 0.375 to 0.391 nm (see Table XII), but then 0.75–1.0 phosphate anions, on the average, are within the first coordination sphere of the metal cation. An X-ray diffraction study of aqueous phosphoric acid yielded distances ranging from 0.360 to 0.373 nm, as its concentration decreased, according to two models that had 4 or 8 water molecules as the nearest neighbors (hydrogen bonded to the phosphate group). A molecular dynamics computer simulation study yielded a very low value for the P–O(water) distance, 0.306 nm, in a small phosphate–water cluster, containing 6–18 water molecules per PO_4^{3-} anion.

Acetate. The acetate anion poses special difficulties, due to its nonsymmetrical nature, having a hydrophilic end and a hydrophobic end. Two X-ray diffraction studies of aqueous divalent metal acetate solutions yielded C(methyl)–O(water) distances of 0.35–0.37 nm, in agreement with a molecular dynamics computer simulation study (Table XII). The latter study also gave the O(carboxylate)–O(water) distance as 0.27 nm.

Sulfate. Many studies of aqueous divalent and trivalent metal sulfate solutions by X-ray diffraction, as well as a few studies of ammonium sulfate and sulfuric acid solutions, yielded rather consistent results and a S–O(water) internuclear distance of $0.381_5 \pm 0.007_1$ nm. The number of nearest water molecule neighbors ranged from 6.4 to 9.6, depending on the fraction of the sulfate anion that was in the inner coordination sphere of the metal cation. Eight hydrogen-bonded nearest neighbors were assumed for the sulfuric acid solutions; see Table XII.

Selenate. Some aqueous trivalent lanthanide selenate solutions were studied by X-ray diffraction, and the Se–O(water) internuclear distance of 0.395 nm, with an assumed number of 8 water nearest neighbors of the selenate anion, was found; see Table XII.

Molybdate and Tungstate. Table XII shows the results from an X-ray diffraction study, using the isomorphous substitution principle, according to which a definite hydration shell exists around these anions, so that a characteristic Mo–water or W–water distance can be discerned in addition to the intraionic Mo–O and W–O distances.

C. Ionic Radii from Interparticle Distances

The mean ion–water distances from Tables I–XII, i.e., the mean internuclear distances between the monoatomic ions or the central atoms of polyatomic ions and the oxygen atoms of the water molecules in their first hydration shells, are collected in Table XIII. Application of eq 9 to these $d_{\text{ion-water}}$ values permits then the evaluation of the radii of the ions in aqueous solutions, R_{ion}, provided that the value of R_{water} is known. A brief discussion of this problem is given in Section III.B, where some of the results for R_{water}[29–33] are summarized. Further determinations of this quantity[216–220] are in essential agreement with the average values quoted previously: $R_{\text{water}} = 0.142_0 \pm 0.000_5$ nm for liquid water at room temperature. However, R_{water} depends on the temperature, as was found by Narten and Levy[29a] in their X-ray diffraction study. Numerical values from this study (the original presented only graphical results) were quoted by Lie et al.[31b] and Stillinger and Rahman[32b] for the range 4–200 °C, which can be fitted to the expression $R_{\text{water}} = 0.1409 + 3.1 \times 10^{-5}(t/°\text{C})$ nm. This linear expression agrees, within the experimental error of 0.002 nm, also with later X-ray diffraction data,[216] neutron diffraction data,[219] and molecular dynamics calculations[32b,220] for temperatures from −4 to +118 °C.

It can be argued, however, that the water in the first hydration shell of an ion is under much stronger forces than those due to the fields prevailing in liquid water. The compressive (electrostrictive) force of the electrical field E near an ion has been translated[221] (see also ref 4, p 104) into values of the pressure prevailing there by means of the differential expression

$$dP = (\epsilon_0/4\pi\kappa_T)(\partial\epsilon/\partial P)_{E,T}\,dE \qquad (21)$$

where κ_T is the isothermal compressibility of water. A molecular dynamics computer simulation of water under such a high pressure that the density of water was 1.3474 g cm^{-3} at 68 °C yielded[220] the value $R_{\text{water}} = 0.140$ nm instead of the 0.143 nm at ambient pressure expected from the above linear expression for this temperature. The same result was obtained for 77 °C at a density of 1.346 g cm^{-3} in a similar study.[222] A neutron diffraction study at 25 °C up to a pressure of 5 kbar (density of 1.485 g cm^{-3}) gave a decrease of R_{water} of 0.025 nm relative to ambient pressure.[223] The electrostriction producing these densities and distances corresponds at 25 °C to an electrical field of 2.2 × 10^{10} V m^{-1} or a distance of 0.09 $z^{1/2}$ nm from the center of an ion,[4] i.e., to a realistic situation. On this basis, the value of R_{water} at room temperature near an ion would be 0.139 nm, with an estimated uncertainty of 0.002 nm.

TABLE XIII. Mean Ion–Water Internuclear Distances (from Tables I–XII), Calculated Ionic Radii in Solution (R_{ion}, eq 9), and Pauling-Type Crystal Ionic Radii, $R^{\text{P}}_{\text{ion}}$

ion	$d_{\text{ion-W}}$/nm	R_{ion}/nm	$R^{\text{P}}_{\text{ion}}$/nm
Li^+	0.208 ± 0.007	0.071 ± 0.007	0.074
Na^+	0.2356 ± 0.0060	0.097 ± 0.006	0.102
K^+	0.2798 ± 0.0081	0.141 ± 0.008	0.138
Rb^+	0.289	0.150	0.149
Cs^+	0.3139 ± 0.0076	0.173 ± 0.008	0.170
Ag^+	0.2417 ± 0.0021	0.102 ± 0.002	0.115
H_3O^+	0.2755 ± 0.0015	0.141 ± 0.002	
Mg^{2+}	0.2090 ± 0.0041	0.070 ± 0.004	0.072
Ca^{2+}	0.2422 ± 0.0052	0.103 ± 0.005	0.100
Sr^{2+}	0.264	0.125	0.125
Mn^{2+}	0.2192 ± 0.0013	0.080 ± 0.001	0.083
Fe^{2+}	0.2114 ± 0.0010	0.072 ± 0.001	0.078
Co^{2+}	0.2106 ± 0.0022	0.072 ± 0.002	0.075
Ni^{2+}	0.2061 ± 0.0014	0.067 ± 0.001	0.069
Cu^{2+} eq	0.1968 ± 0.0047		
Cu^{2+} ax	0.240 ± 0.010		
Cu^{2+} mean	0.211	0.072	0.073
Zn^{2+}	0.2098 ± 0.0066	0.070 ± 0.007	0.075
Cd^{2+}	0.2301 ± 0.0025	0.091 ± 0.003	0.095
Hg^{2+}	0.242	0.103	0.102
Sn^{2+}	0.233	0.094	0.093
Al^{3+}	0.1887 ± 0.0015	0.050 ± 0.002	0.053
Y^{3+}	0.2365	0.097	0.101
La^{3+}	0.2528 ± 0.0048	0.114 ± 0.005	0.118
Ce^{3+}	0.255	0.116	0.114
Pr^{3+}	0.254	0.115	0.114
Nd^{3+}	0.2472 ± 0.0033	0.108 ± 0.003	0.112
Sm^{3+}	0.2448 ± 0.0021	0.106 ± 0.002	0.109
Eu^{3+}	0.245	0.106	0.107
Gd^{3+}	0.239	0.100	0.106
Tb^{3+}	0.2403 ± 0.0005	0.101 ± 0.001	0.104
Dy^{3+}	0.2370 ± 0.0003	0.098 ± 0.001	0.103
Er^{3+}	0.2363 ± 0.0005	0.097 ± 0.001	0.100
Tm^{3+}	0.236	0.097	0.099
Lu^{3+}	0.234	0.095	0.097
Cr^{3+}	0.1969 ± 0.0032	0.058 ± 0.003	0.062
Fe^{3+}	0.2031 ± 0.0019	0.064 ± 0.002	0.065
Rh^{3+}	0.204 ± 0.001	0.065 ± 0.001	
In^{3+}	0.2156 ± 0.0002	0.076 ± 0.001	0.079
Tl^{3+}	0.2231 ± 0.0005	0.084 ± 0.001	0.088
Th^{4+}	0.253	0.114	0.106
F^-	0.2630 ± 0.0025	0.124 ± 0.003	0.133
Cl^-	0.3187 ± 0.0067	0.180 ± 0.007	0.181
Br^-	0.3373 ± 0.0054	0.198 ± 0.005	0.196
I^-	0.3647 ± 0.0036	0.225 ± 0.004	0.220
NO_3^- ax	0.265		
NO_3^- eq	0.3451 ± 0.0043		
NO_3^- mean	0.316 ± 0.002	0.177 ± 0.002	0.179
ClO_4^-	0.370	0.241	0.240
$H_2PO_4^-$	0.377 ± 0.011	0.238 ± 0.011	0.238
SO_4^{2-}	0.3815 ± 0.0071	0.242 ± 0.007	0.230
SeO_4^{2-}	0.395	0.256	0.243
$Mo(W)O_4^{2-}$	0.406	0.267	0.254–0.270

Application of eq 9 with this value of R_{water} yields the values of R_{ion} listed in the third column of Table XIII. The uncertainty given reflects that of $d_{\text{ion-water}}$ in the second column, not compounded by that of R_{water}. These values are compared in both Table XIII and Figure 2 with the values of $E^{\text{P}}_{\text{ion}}$, the Pauling-type

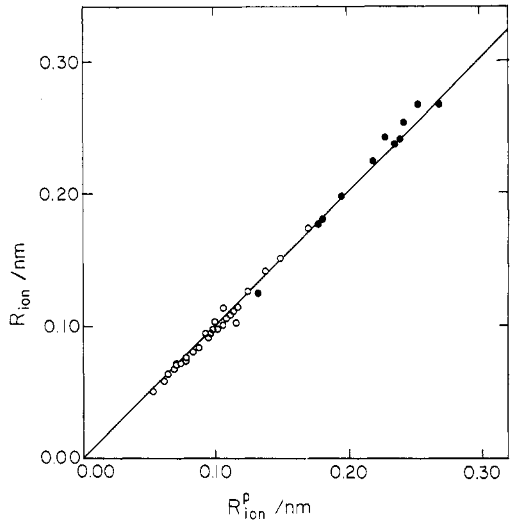

Figure 2. Ionic radii in solution, $R_{ion} = d_{ion-water} - R_{water}$ with $R_{water} = 0.139_3$ nm, as a function of the Pauling-type crystal ionic radii, R^P_{ion}, for coordination number 6 (except for Sr, Y, the lanthanides, and Th, where R^P_{ion} for coordination number 8 are used). Open circles, cations; filled circles, anions.

crystal ionic radii of the monoatomic ions for coordination number 6. These latter values were taken from Shannon and Prewitt,[20] except for Sn^{2+}, Cl^-, Br^-, and I^-, for which the values of Ahrens[21] were taken. The values for Sr^{2+}, Y^{3+}, the lanthanides, and Th^{4+} are for coordination number 8.[20] Values given in the column R^P_{ion} for polyatomic ions are thermochemical-type radii from Marcus and Loewenschuss.[26]

Good agreement between the R_{ion} and R^P_{ion} values in the third and fourth columns of Table XIII is noted in most cases (see also Figure 2). Noteworthy exceptions are Ag^+, F^-, SO_4^{2-}, and SeO_4^{2-}. A possible reason for the disagreement in the case of Ag^+ is that the applicable coordination number is not 6, but the R^P_{ion} = 0.102 nm for a square-planar coordination[20] is the appropriate one also for the solution. A similar expanation, i.e., a much lower coordination number than 6 for F^- in the solution to account for the low value R_{ion} = 0.124 nm is unlikely, however. In the cases of sulfate and selenate the possible reasons for the discrepancies could be wrong estimates of the thermochemical radii, since the lattice energies of salts of these anions are not known accurately enough. It should be noted that in the case of Li^+ the radius is between the average value in the solution, 0.206 nm, and the crystal ionic radius for coordination number 6. If a coordination number of 4 were selected, then the agreement would be between R^P_{ion} = 0.059 nm and $d_{ion-water}$ = 0.198 nm, which agrees well with data shown in Table I and Figure 1 (for low water-to-salt ratio). Therefore the question of what the "real" radius of Li^+ in dilute aqueous solutions remains open.

Another complication that ought to be considered is the fact that the water molecule is not spherical and that in the first hydration sphere it directs a hydrogen atom toward anions, forming a hydrogen bond, whereas it directs its oxygen atom toward cations. How this affects the applicable R_{water} is impossible to ascertain from simple considerations. The geometry of the orientation of the nearest water molecules to certain ions (Li^+, Ni^{2+}, and Cl^-, for instance) has been determined by the FODNS technique[35,36] (see section IV.A.2), so that the internuclear distances ion–hydrogen atom (deuterium atom) are known. Still, this does not permit the apportioning of this distance between the ion and the water molecule. The agreement between R_{ion} and R^P_{ion} for most of the anions (Table XIII) does indicate that the average value of R_{water} = 0.139 nm is a reasonable compromise for both cations and anions.

VI. Ionic Radii in Nonaqueous Solvents

Work on the sizes of ions and solvent molecules in nonaqueous solvents is much less extensive than the corresponding work on water and aqueous ionic solutions. One reason for this is, obviously, the greater general importance of water and aqueous solutions. Another reason is technical in nature, however, and is the larger number of atoms, compared with water, in the nonaqueous solvents. With this larger number, there are more intramolecular distances that must be accounted for in the X-ray or neutron diffraction results, and suitable interaction models required for the computer simulations are that much more complicated.

Compared with the large body of information on the structure of liquid water,[29-32,216-220,222,223] from which R_{water} required in eq 9 can be obtained, there is only a limited body for nonaqueous solvents of electrolytes. (Structural information on so-called "inert" solvents such as 2,2-dimethylpropane, benzene, chloroform, and carbon tetrachloride is not relevant in the present context.) Following is a brief and nonexhaustive presentation of the sizes found for nonaqueous solvents by the more recent diffraction and computer simulation methods. Except for HF and NH_3, methanol and formamide have the simplest molecules and have received the most attention in this respect.

A neutron diffraction study of DF at 20 °C found in the chain-like aggregates (two nearest neighbors) the hydrogen-bonded F–F internuclear distance to be 0.256 nm.[224] Half of this can be taken to be the mean radius of anhydrous hydrogen fluoride. Liquid ammonia was studied by the molecular dynamics method at 196 K, near its triple point,[225] by neutron diffraction at 208 and 295 K (22 °C),[226] and by X-ray diffraction at 277 K (4 °C).[227] The very short hydrogen-bonded N–N internuclear distance of 0.227 nm was found at the lowest temperature, but only much higher distances, 0.34 and 0.37 nm, were compatible with the neutron and X-ray diffraction data at the higher temperatures. Of the 12 neighbors a central ammonia molecule has, about 6 are at the nearer distance and 6 at the farther one. The mean radius of an ammonia molecule in the room temperature liquid is thus ≥0.17 nm.

The structure of liquid formamide was studied by means of X-ray diffraction[228-232] and neutron and electron diffraction.[229] In the earliest X-ray diffraction study[228] the hydrogen-bonded O–N internuclear distance was 0.305 nm; in a later study by all three diffraction techniques[229] a somewhat shorter distance, 0.290 nm, was found. The nature of the aggregates, whether chainlike, rings, or both, could not be determined unequivocally, but the presence of both kinds of aggregates seems now to be the more probable case.[232] Since the formamide molecule is not spherical, it is difficult to see whether a radius can be assigned on the basis of this O–N distance. However, the ability of the solvent to approach cations (with the oxygen atom toward the ion) and anions (with the N-bonded hydrogen atom toward the ion) to certain distances is another question, and probably one-half of the O–N distance is not the answer. In liquid *N*-methylformamide X-ray diffraction indicated the presence of a flexible linear chain structure, which was confirmed by ab initio molecular orbital calculations.[233] In *N*,*N*-dimethylformamide a similar study indicated the absence of any significant structure.[234]

Liquid methanol has been subjected to several studies, both by Monte Carlo computer simulation[235,236] and by X-ray[237,238] and neutron[239] diffraction. Chainlike aggregates are the main species, with hydrogen-bonded O–O internuclear distances of 0.281 nm[235] and an average of 1.85 neighbors per molecule (i.e., the chains are sufficiently short for terminal molecules, with only one neighbor, to contribute significantly to the average). Increased pressure increases the number of neighbors appreciably but decreases the distances only slightly.[236] Somewhat shorter distances were obtained by the X-ray diffraction method: 0.278 nm with only an average of 1.5 neighbors[237] or, in a study with higher accuracy at 20 °C,[238] $0.279_8 \pm 0.000_6$ nm with an average of $1.7_7 \pm 0.0_7$ neighbors. The neutron diffraction study[239] assigned 0.285 nm to this distance in the attempted fit of the data. The nonsphericity of the molecule prevents the interpretation of the O–O distance in terms of a molecular radius, but one-half of this distance, 0.140 nm, appears to be the distance to which a solvent molecule can approach an ion (without taking into account the electrostriction; see section V.C). In two studies of ethanol, somewhat larger hydrogen-bonded O–O distances were found: 0.285 nm with 1.9 neighbors in the chain from Monte Carlo calculations[235] and $0.280_8 \pm 0.000_8$ nm with $1.8_1 \pm 0.0_8$ neighbors from X-ray diffraction at 20 °C.[238] In *tert*-butyl alcohol (2-methyl-2-propanol) a somewhat shorter O–O distance, 0.274 nm, was found by X-ray diffraction at 26 °C, slightly above the melting point.[240] The same comment concerning the radius and the approach to ions made for methanol applies also for the other alcohols. In an X-ray and neutron diffraction study of liquid formic acid the average mutual configuration of the C=O bonds in two neighboring molecules was determined, but no data were given from which an average radius for this solvent could be obtained.[241]

An X-ray diffraction study of acetonitrile at 20 °C gave the center-to-center distance between a central molecule and each of its four nearest neighbors as 0.38 nm.[242] Since, again, acetonitrile is not a spherical but an elongated molecule, it is not immediately obvious how this distance relates to the distance of approach of the solvent to an ion.

A brief discussion of structural information on nonaqueous solutions of ions, from which ion–solvent internuclear distances and hence ionic radii can be estimated, follows. No effort was made to scan the literature on this subject exhaustively.

A neutron diffraction study[226] of a concentrated ^{7}Li–ND_3 solution (having 4 ND_3 molecules per Li atom) at 216 K indicated the presence of a Li–N internuclear distance of 0.2 nm and a Li–D distance of 0.25 nm. If the electron is delocalized in this solution, the lithium is ionized to Li^+, so that the former distance is relevant to this review. An EXAFS study[243] of rubidium in ammonia in the temperature range 213–283 K and NH_3/Rb ratios of 8–160 indicated the presence of Rb^+ ions with 6 ammonia molecules in the first solvation shell, at an Rb–N internuclear distance of 0.30_9 nm. A similar study[244] of ytterbium in ammonia solutions with 15.6, 151, or 294 NH_3 per Yb found a first solvation shell with n slightly >6 and an Yb–N internuclear distance of 0.262 ± 0.002 nm. The ytterbium was in the Yb^{2+} state. A Monte Carlo simualtion study[245] of a solution of Na^+ in 18.45 mol % ammonia in water solution (206 solvent molecules per Na^+) indicated the presence of 2.4 water and 4.0 ammonia molecules in the first solvation shell. The Na–N internuclear distance was taken as 0.235 nm from an ab initio calculation.

An early X-ray diffraction study[228] of KI in formamide at 5.3–31.1 mol of solvent per mol of salt indicated the presence of 2.1–4.6 solvent molecules in the first solvation shell of the K^+ ion in this concentration range, at a K–O internuclear distance of about 0.30 nm. In spite of the high relative permittivity of formamide, extensive ion pairing was postulated to occur in the solutions. Another X-ray diffraction study[246] dealt with LiCl in formamide with 4.0 mol of solvent per mol of salt. It was found that the Li^+ cation has preferentially the O atom of formamide as its nearest neighbor, at a Li–O distance of 0.224 ± 0.002 nm and $n = 5.4 \pm 0.3$ and that for the Cl anion it is the hydrogen-bonded N atom that solvates it, at a Cl–N distance of 0.327 ± 0.002 nm and $n = 4.5 \pm 0.1$.

An electron diffraction study[247] of $ZnBr_2$ in the presence of about equimolar LiBr in *N*,*N*-dimethylformamide (DMF) at 6.27 mol of solvent per mol of $ZnBr_2$ indicated the presence of $ZnBr_3^-$ as the major species but that the solvent was still present in the first solvation shell, with a Zn–O internuclear distance of 0.222 nm. An X-ray diffraction study[248] of Cd(II) in DMF showed $n = 6$ and Cd–O internuclear distances of 0.2296 nm. A recent X-ray diffraction study[249] showed that Cu(II) cations in *N*,*N*-dimethylformamide are located in the center of a distorted octahedron, with equatorial Cu–O distances of 0.203 nm and axial ones of 0.243 nm (cf. the situation in aqueous solutions (Table VII)). When acetonitrile is added (to a mole ratio of 2 per 1 DMF), the axial DMF solvent molecules are removed, but no acetonitrile ones replace them at distances that can be considered as inside the solvation shell. The structure of the Cu(II) solvation shell in pure acetonitrile could not be studied by X-ray diffraction, due to the low solubility of $Cu(ClO_4)_2$ in this solvent.[249] However, an EXAFS study[250] of $CuBr_2$ in acetonitrile, without and with added LiBr, showed definite solvation of Cu(II) by acetonitrile, with a Cu–N internuclear distance of 0.203 nm, but with Br^- anions also present in the first solvation shell.

In dimethyl sulfoxide, an X-ray diffraction study[248] showed that both Cd(II) and Hg(II) formed hexasolvates in the first solvation shell, with cation–O internuclear distances of 0.2292 and 0.2393 nm, respectively. An X-ray diffraction study[251] of $ZnBr_2$ in acetone (4.07 mol of acetone per mol of salt) indicated bromide anions to be present in the first solvation shell and a Br–O internuclear distance of 0.32 nm, but no Zn–O distance was reported.

Salt solutions in methanol received considerably more attention than solutions in other solvents. In early studies of Wertz and Kruh[27,125,252] cobalt(II) chloride and bromide and iron(III) chloride solutions in methanol were studied by X-ray diffraction. The Cl–O and Br–O internuclear distances were found to be the same as in aqueous solutions, 0.31 nm[27,252] and 0.325 nm,[125] respectively. In the latter case, also a Co–O distance of about 0.20 nm could be estimated for a species that is tetrahedral, with two bromide and two methanol ligands around the cobalt atom. Lind[182] interpreted the data for $FeCl_3$ as indicating the presence of $FeCl_2(solvent)_4^+$ species (beside $FeCl_4^-$) with Fe–O distances of 0.207 nm in both water and methanol. A Monte Carlo computer simulation of sodium methoxide in methanol,[253] with 127 solvent molecules per ion, showed that for Na^+ $n = 6$ and the Na–O internuclear distance is 0.232 ± 0.003 nm and for CH_3O^- $n = 5$ with the O–O distance 0.267 nm. An X-ray diffraction study[254] of $CuCl_2$, at 7.1–23.1 mol of methanol per mol of salt, indicated the presence of the species $Cu(Cl_{eq})_2(CH_3OH_{eq})_2(CH_3OH_{ax})_2$, with Cu–O internuclear distances of 0.194 nm for the equatorial and 0.246_5 nm for the axial solvent molecules. An X-ray study[255] of $MgCl_2$ in methanol (18.7 mol of solvent per mol of salt) showed the regular octahedral arrangement of methanol around the Mg^{2+} cation with a Mg–O internuclear distance of 0.206 nm, and for Cl^- $n = 6$ also, but not necessarily highly symmetrical, with a Cl–O distance of 0.315 nm. The ion–C distances were also given, so that the geometry of the solvent around the ions can also be inferred. A recent EXAFS study[256] of $CoBr_2$ in methanol showed that $CoBr(CH_3OH)_5^+$ is the predominant species in concentrated solutions, but at 0.1 mol dm^{-3} the hexasolvate predominates, with Co–O distances of 0.208 nm. In ethanol at 0.2 mol dm^{-3} and higher concentrations the predominant species is $CoBr_2(C_2H_5OH)_2$, with Co–O distances decreasing from 0.206 to 0.203 nm as the concentration increases to 3.83 mol dm^{-3}. An earlier X-ray diffraction study[27] of a $CoBr_2$ solution in ethanol of a similar high concentration (3.81 mol kg^{-1}) gave only the Cl–O distance, 0.31 nm, the same as in methanol or water.

VII. Concluding Remarks

The question was raised in the discussion of the concept of ionic radii (section III.A) whether the internuclear distances $d_{\text{ion-water}}$ between ions (or the central atoms of polyatomic ions) and water molecules (i.e., the oxygen atom of the water molecule) in their first solvation shell can be determined accurately. The answer to this question was yes: section IV presented the diffraction and computer simulation methods, and section V (Tables I–XII) gave the results that have been obtained. These are summarized in Table XIII. The other question that was raised pertained to the allocation of these distances into the part that "belongs" to the water molecule, R_{water}, and the part that "belongs" to the ion, R_{ion}, i.e., the ionic radius. The answer to that was a qualified yes: if the average, electrostricted value of 0.139_3 nm was used for R_{water}, then values of R_{ion} were obtained that agreed well with the Pauling-type crystal ionic radii for coordination number 6, R^{P}_{ion}. Some specific exceptions were explained ad hoc by the necessity to use R^{P}_{ion} values for other coordination numbers. The general conclusion from this is that Pauling-type crystal ionic radii may serve well for the radii of ions in solution for all the applications for which examples were shown in section II.

Some questions, however, still remain open. One that has already been touched upon in section V.C is whether the same value of R_{water} applies for cations and anions, in view of the different orientation of the water molecule toward them. Another question is whether the internuclear distances $d_{\text{ion-water}}$ are temperature and pressure dependent, and if so, how much. Many of the diffraction measurements and the computer simulations were made at a specified temperature, usually 20 or 25 °C, but in many other cases only "room temperature" or the like was specified, if at all.

A few determinations were made at several specified temperatures. For instance, aqueous cadmium sulfate was studied[158] by X-ray diffraction at 9 and 62 °C, but $d_{\text{ion-water}}$ was determined to only ±0.001 nm. The small differences noted between the results at these temperatures are probably not significant and could arise from the different number of sulfate ions in the first coordination shell of the cadmium ion at the two temperatures, and not from inherent temperature sensitivity of the free ion–solvent distance. An EXAFS study[145] of some aqueous divalent metal halides at temperatures between 20 and 75 °C indicated that no change in n takes place in this range, and presumably also none in $d_{\text{ion-water}}$. A Monte Carlo computer simulation study[257] explored the difference in the radial distribution functions of water around Li^+, Na^+, K^+, F^-, and Cl^- between 25 and 75 °C at a ratio of 64 water molecules per ion. The height of the first peak in the $g_{\text{ion-water}}(r)$ curve for Li^+, Na^+, and F^- decreases with increasing temperatures (as for pure water), but its position is independent of the temperature. On the contrary, the peak heights for K^+ and Cl^- increase slightly with the temperature, as do their r values. In another Monte Carlo study[258] the thermal ellipsoids of the water molecules surrounding octahedrally a Zn^{2+} cation were determined at 25 °C with 215 water molecules per zinc ion. In yet another computer simulation study,[259] this time by the molecular dynamics method, the effect of pressure, 10 kbar, in $d_{\text{ion-water}}$ was determined for the system involving $1\ Na^+ + 1\ Cl^- + 25\ H_2O$ at 25 °C. No change in the Na–O distances was noted, but the Cl–O distance decreased slightly at the higher pressure. The value of n for Na^+, however, increased from 5.8 to 6.3 as the pressure increased from ambient to 10 kbar. No generalizations can be drawn from these rather sporadic, nonsystematic, studies.

One final remark is in place here: the diffraction measurements (by X-rays, neutrons, or electrons or by the EXAFS method) and the computer simulations (by molecular dynamics and Monte Carlo methods) are applied to electrolyte solutions in only a relatively small number of laboratories. The same names reappear in the publications: see the relevant references 45–259. The most active groups are located in Italy (those of Caminiti, Magini, Clementi, and their respective co-workers), Germany (that of Heinzinger and co-workers), England (that of Enderby, Neilson, and co-workers), Hungary (that of Palinkas and co-workers), Sweden (that of Johansson and co-workers), Japan (that of Ohtaki and co-workers), while several additional groups made important contributions, too. Remarkable, however, is the constant cooperation between many of these groups, co-workers from one being temporary guests with another, so that many of the papers bear addresses of several laboratories. A community of researchers with interest in this field appears to have been built up with worldwide connections, a very commendable development.

Acknowledgments. This work was supported in part by Grant No. 84-00292 from the U.S.-Israel Binational Science Foundation.

VIII. References

(1) Stokes, R. H. *J. Am. Chem. Soc.* **1964**, *86*, 979.
(2) Rashin, A. A.; Honig, B. *J. Phys. Chem.* **1985**, *89*, 5588.
(3) Marcus, Y. *J. Solution Chem.* **1983**, *12*, 271.
(4) Marcus, Y. *Ion Solvation*; Wiley: Chichester (UK), 1986; p 113.
(5) Marcus, Y. *Pure Appl. Chem.* **1987**, *59*, 1093.
(6) Abraham, M. H.; Marcus, Y. *J. Chem. Soc., Faraday Trans. 1* **1986**, *82*, 3255.
(7) Millero, F. J. *Chem. Rev.* **1971**, *71*, 147.
(8) Marcus, Y.; Loewenschuss, A. *Annu. Rep. C, 1984, R. Soc. Chem. (London)* **1985**, 81.
(9) Burgess, J. *Metal Ions in Solution*; Ellis Horwood: Chichester (UK), 1978; Chapter 11.
(10) Eigen, M. *Z. Phys. Chem. (Frankfurt/Main)* **1964**, *1*, 176.
(11) Nightingale, E. R. *J. Phys. Chem.* **1959**, *63*, 1381.
(12) Hertz, H. G.; Spaltoff, W. *Z. Elektrochem.* **1959**, *63*, 1096.
(13) Hertz, H. G. *Ber. Bunsenges. Phys. Chem.* **1963**, *67*, 311.
(14) Blandamer, M. J.; Griffiths, T. R.; Shields, L.; Symons, M. C. R. *Trans. Faraday Soc.* **1964**, *60*, 1524.
(15) Plowman, K. R.; Lagowski, J. J. *J. Phys. Chem.* **1974**, *78*, 143.
(16) Maxey, B. W.; Popov, A. I. *J. Am. Chem. Soc.* **1967**, *89*, 2230.
(17) Coetzee, J. F.; Sharpe, W. R. *J. Solution Chem.* **1972**, *1*, 77.
(18) Goldschmidt, V. M. *Skr. Norske Vid. Akad. Oslo, Math. Nat. Kl.* 1926, *No. 2*; *Ber.* **1927**, *60*, 1263.
(19) Pauling, L. *J. Am. Chem. Soc.* **1927**, *49*, 765; *Nature of the Chemical Bond*, 3rd ed.; Cornell University Press: Ithaca, NY, 1960; Chapter 13.
(20) Shannon, R. D.; Prewitt, C. T. *Acta Crystallogr., Sect. B* **1969**, *25*, 925; **1970**, *26*, 1046.
(21) Ahrens, L. H. *Geochim. Cosmochim. Acta* **1952**, *2*, 155.
(22) Gourary, B. S.; Adrian, F. J. *Solid State Phys.* **1960**, *10*, 128.
(23) Kapustinskii, A. F.; Yatsimirskii, K. B. *Zh. Obshch. Khim.* **1949**, *19*, 2191. Kapustinskii, A. F. *Q. Rev., Chem. Soc.* **1956**, *10*, 283.
(24) Yatsimirskii, K. B. *Izv. Akad. Nauk SSSR, Ot. Khim. Nauk* **1947**, 453; **1948**, 398.
(25) Jenkins, H. B. D.; Thakur, K. P. *J. Chem. Educ.* **1979**, *56*, 576.
(26) Marcus, Y.; Loewenschuss, A. *Annu. Rep. C, 1984, R. Soc. Chem. (London)* **1985**, 81.
(27) Levy, H. A.; Danford, M. D. In *Molten Salt Chemistry*; Blander, M., Ed.; Wiley: New York, 1964; Chapter 2.
(28) Marcus, Y. *Introduction to Liquid State Chemistry*; Wiley: Chichester (UK), 1977; p 121.
(29) (a) Narten, A. H.; Levy, H. A. *J. Chem. Phys.* **1971**, *55*, 2263. (b) Narten, A. H. *Ibid.* **1972**, *56*, 5681.
(30) Kalman, E.; Lengyel, S.; Haklik, L.; Eke, E. *J. Appl. Crystallogr.* **1974**, *7*, 442.
(31) (a) Lie, G. C.; Clementi, E. *J. Chem. Phys.* **1975**, *62*, 2195. (b) Lie, G. C.; Clementi, E.; Yoshimine, M. *Ibid.* **1976**, *64*, 2314.
(32) (a) Rahman, A.; Stillinger, F. H. *J. Chem. Phys.* **1971**, *55*, 3336. (b) Stillinger, F. H.; Rahman, A. *Ibid.* **1974**, *60*, 1545.
(33) Lonsdale, K. *Proc. R. Soc. (London), A* **1958**, *A247*, 424.
(34) Kruh, R. F. *Chem. Rev.* **1962**, *62*, 319.
(35) Soper, A. K.; Neilson, G. W.; Enderby, J. E.; Howe, R. A. *J. Phys. (C), Solid State Phys.* **1977**, *10*, 1793.
(36) Enderby, J. E.; Neilson, G. W. *Rep. Prog. Phys.* **1981**, *44*, 593.
(37) Annis, B. K.; Hahn, R. L.; Narten, A. H. *J. Chem. Phys.* **1985**, *82*, 2086.
(38) Licheri, G.; Pinna, G. *EXAFS and Near Edge Structure*; Bianconi, A., Incoccia, L., Stipcich, S., Eds.; *Springer Ser. Chem. Phys.* **1983**, *27*, 240.
(39) Kalman, E.; Serke, I.; Palinkas, G.; Johansson, G.; Kabisch, G.; Maeda, M.; Ohtaki, H. *Z. Naturforsch.* **1983**, *A38*, 225.
(40) Heinzinger, K. *Physica B & C* **1985**, *131*, 196.
(41) Kong, C. L. *J. Chem. Phys.* **1973**, *59*, 2464.
(42) Alagona, G.; Ghio, C.; Kollman, P. *J. Am. Chem. Soc.* **1986**, *108*, 185.
(43) Briand, C. L.; Burton, J. J. *J. Chem. Phys.* **1976**, *64*, 2888. (a) Ozutsumi, K.; Ohtaki, H.; Kusumegi, A. *Bull. Chem. Soc. Jpn.* **1984**, *57*, 2612.
(44) Malenkov, G. G.; Dyakonova, L. P.; Brizhik, L. S. *VINITI* 1980, 346-80.
(45) Yamaguchi, T.; Ohtaki, H.; Spohr, E.; Palinkas, G.; Heinzinger, K.; Probst, M. M. *Z. Naturforsch.* **1986**, *A41*, 1175.
(46) Hewish, N. A.; Neilson, G. W.; Enderby, J. E. *Nature (London)* **1982**, *297*, 138.
(47) Bounds, D. G. *Mol. Phys.* **1985**, *54*, 1335.
(48) Yamaguchi, T.; Lindqvist, O.; Claeson, T.; Boyce, J. B. *Chem. Phys. Lett.* **1982**, *93*, 528.
(49) Narten, A. H.; Vaslow, F.; Levy, H. A. *J. Chem. Phys.* **1973**, *58*, 5017.
(50) Licheri, G.; Piccaluga, G.; Pinna, G. *J. Appl. Crystallogr.* **1973**, *6*, 392.
(51) Heinzinger, K. *Pure Appl. Chem.* **1985**, *57*, 1031.
(52) Impey, R. W.; Madden, P. A.; McDonald, I. R. *J. Phys. Chem.* **1983**, *87*, 5071.
(53) Marchese, F. T.; Beveridge, D. L. *J. Am. Chem. Soc.* **1984**, *106*, 3713.
(54) Bopp, P.; Okada, I.; Ohtaki, H.; Heinzinger, K. *Z. Naturforsch.* **1985**, *A40*, 116.
(55) Szasz, Gy. I.; Heinzinger, K.; Riede, W. O. *Z. Naturforsch.* **1981**, *A36*, 1067.
(56) Heinzinger, K. *Stud. Phys. Theor. Chem.* **1983**, *27*, 61.
(57) Radnai, T.; Heinzinger, K.; Szasz, Gy. I. *Z. Naturforsch.* **1981**, *A36*, 1076.
(58) Paschina, G.; Piccaluga, G.; Pinna, G.; Magini, M. *Chem. Phys. Lett.* **1983**, *98*, 157.
(59) Musinu, A.; Paschina, G.; Piccaluga, G.; Magini, M. *J. Chem. Phys.* **1984**, *80*, 2772.
(60) Mezei, M.; Beveridge, D. L. *J. Chem. Phys.* **1981**, *74*, 6902.
(61) Ergin, Yu. V.; Koop, O. Ya.; Khrapko, A. M. *Zh. Fiz. Khim.* **1979**, *53*, 2109.
(62) Okada, I.; Kitsuno, Y.; Lee, H.-G.; Ohtaki, H. *Stud. Phys. Theor. Chem.* **1983**, *27*, 81.
(63) Okada, I.; Kitsuno, Y.; Lee, H.-G.; Ohtaki, H. *Abstr. VI Int. Symp. Solute-Solute-Solvent Interact., Minoo* **1982**, p 1A-M07.
(64) Newsome, J. R.; Neilson, G. W.; Enderby, J. E. *J. Phys. C: Solid State Phys.* **1980**, *13*, L923.
(65) Palinkas, G.; Radnai, T.; Hajdu, F. *Z. Naturforsch.* **1980**, *A35*, 107.
(66) Ohtomo, N.; Arakawa, K. *Bull. Chem. Soc. Jpn.* **1979**, *52*, 2755.
(67) Licheri, G.; Piccaluga, G.; Pinna, G. *Chem. Phys. Lett.* **1975**, *35*, 119.
(68) Heinzinger, K.; Vogel, P. C. *Z. Naturforsch.* **1976**, *A31*, 463.
(69) Szasz, Gy. I.; Heinzinger, K.; Palinkas, G. *Chem. Phys. Lett.* **1981**, *78*, 194.
(70) Kistenmacher, H.; Popkie, H.; Clementi, E. *J. Chem. Phys.* **1974**, *61*, 799.
(71) Clementi, E.; Barsotti, R. *Chem. Phys. Lett.* **1978**, *59*, 21.
(72) Ohtomo, N.; Arakawa, K. *Bull. Chem. Soc. Jpn.* **1980**, *53*, 1789.
(73) Caminiti, R.; Licheri, G.; Piccaluga, G.; Pinna, G. *Rend. Sem. Fac. Sci. Cagliari* 1977, *XLVI, Suppl. 19*.
(74) Vogel, P. C.; Heinzinger, K. *Z. Naturforsch.* **1976**, *A31*, 476.
(75) Palinkas, G.; Riede, W. O.; Heinzinger, K. *Z. Naturforsch.* **1977**, *A32*, 1137.
(76) Bopp, P.; Dietz, W.; Heinzinger, K. *Z. Naturforsch.* **1979**, *A34*, 1424.
(77) Maeda, M.; Ohtaki, H. *Bull. Chem. Soc. Jpn.* **1975**, *48*, 3755.
(78) Caminiti, R.; Licheri, G.; Paschina, G.; Piccaluga, G.; Pinna, G. *J. Chem. Phys.* **1980**, *72*, 4522.
(79) Limtakrul, J. P.; Rode, B. M. *Monatsh. Chem.* **1985**, *116*, 1377.
(80) Brady, G. W. *J. Chem. Phys.* **1958**, *28*, 464.
(81) Neilson, G. W.; Skipper, N. *Chem. Phys. Lett.* **1985**, *114*, 35.
(82) Terekhova, D. S.; Ryss, A. I.; Radchenko, I. V. *J. Struct. Chem.* **1969**, *10*, 807.
(83) Eck, C. L. van P. van; Mendel, H.; Boog, W. *Discuss. Faraday Soc.* **1957**, *24*, 200, 235.
(84) Szasz, Gy. I.; Heinzinger, K. *Z. Naturforsch.* **1983**, *A38*, 214.
(85) Szasz, Gy. I.; Heinzinger, K. *Z. Naturforsch.* **1979**, *A34*, 840.
(86) Lawrence, R. M.; Kruh, R. F. *J. Chem. Phys.* **1967**, *47*, 4758.
(87) Bertagnolli, H.; Weidner, J.-U.; Zimmermann, H. W. *Ber. Bunsenges. Phys. Chem.* **1974**, *78*, 2.
(88) Maeda, M.; Maegawa, Y.; Yamaguchi, T.; Ohtaki, H. *Bull. Chem. Soc. Jpn.* **1979**, *52*, 2545.
(89) Sandstrom, M.; Neilson, G. W.; Johansson, G.; Yamaguchi, T. *J. Phys. C: Solid State Phys.* **1985**, *18*, L1115.
(90) Yamaguchi, T.; Lindqvist, O.; Boyce, J. B.; Claeson, T. *Acta Chem. Scand.* **1984**, *A38*, 423.
(91) Yamaguchi, T.; Johansson, G.; Holmberg, B.; Maeda, M.; Ohtaki, H. *Acta Chem. Scand.* **1984**, *A38*, 437.
(92) Ohtomo, N.; Arakawa, K.; Takeuchi, M.; Yamaguchi, T.; Ohtaki, H. *Bull. Chem. Soc. Jpn.* **1981**, *54*, 1314.
(93) Caminiti, R. *Chem. Phys. Lett.* **1983**, *96*, 390.
(94) Caminiti, R.; Cucca, P. *Chem. Phys. Lett.* **1984**, *108*, 51.
(95) Lee, H.-G.; Matsumoto, Y.; Yamaguchi, T.; Ohtaki, H. *Bull. Chem. Soc. Jpn.* **1983**, *56*, 443.
(96) Caminiti, R.; Atzei, D.; Cucca, P.; Squintu, F.; Bongiovanni, G. *Z. Naturforsch.* **1985**, *A40*, 1319.

(97) Hewish, N. A.; Neilson, J. E. *Chem. Phys. Lett.* **1981**, *84*, 425.
(98) Bol, W.; Gerrits, G. J. A.; Eck, C. L. van P. van *J. Appl. Crystallogr.* **1970**, *3*, 486.
(99) Caminiti, R. *J. Mol. Liq.* **1984**, *28*, 191.
(100) Dietz, W.; Riede, W. O.; Heinzinger, K. *Z. Naturforsch.* **1982**, *A37*, 1038.
(101) Palinkas, G.; Radnai, T.; Dietz, W.; Szasz, Gy. I.; Heinzinger, K. *Z. Naturforsch.* **1982**, *A37*, 1049.
(102) Caminiti, R. *Chem. Phys. Lett.* **1982**, *88*, 103.
(103) Caminiti, R.; Cucca, G.; Monduzzi, M.; Saba, G.; Crisponi, G. *J. Chem. Phys.* **1984**, *81*, 543.
(104) Caminiti, R.; Licheri, G.; Piccaluga, G.; Pinna, G. *J. Appl. Crystallogr.* **1979**, *12*, 34.
(105) Caminiti, R.; Licheri, G.; Piccaluga, G.; Pinna, G. *Chem. Phys. Lett.* **1979**, *61*, 45.
(106) Albright, J. N. *J. Chem. Phys.* **1972**, *56*, 3783.
(107) Ryss, A. I.; Radchenko, I. V. *J. Struct. Chem.* **1965**, *6*, 422.
(108) Dorosh, A. K.; Skrychevskii, A. F. *J. Struct. Chem.* **1964**, *5*, 842.
(109) Caminiti, R.; Licheri, G.; Piccaluga, G.; Pinna, G. *Chem. Phys. Lett.* **1977**, *47*, 275.
(110) Probst, M. M.; Radnai, T.; Heinzinger, K.; Bopp, P.; Rode, B. M. *J. Phys. Chem.* **1985**, *89*, 753.
(111) Licheri, G.; Piccaluga, G.; Pinna, G. *J. Chem. Phys.* **1976**, *64*, 2437.
(112) Cummings, S.; Enderby, J. E.; Howe, R. A. *J. Phys. C: Solid State Phys.* **1980**, *13*, 1.
(113) Licheri, G.; Piccaluga, G.; Pinna, G. *J. Chem. Phys.* **1975**, *63*, 4412.
(114) Shapovalov, I. M.; Radchenko, I. V. *J. Struct. Chem.* **1971**, *12*, 705.
(115) Caminiti, R.; Musinu, A.; Paschina, G.; Pinna, G. *J. Appl. Crystallogr.* **1982**, *15*, 482.
(116) Licheri, G.; Pinna, G. *EXAFS and Near Edge Structure*; Bianconi, A., Incoccia, L., Stipcich, S., Eds.; *Springer Ser. Chem. Phys.* **1983**, *27*, 240.
(117) Caminiti, R.; Marongin, G.; Paschina, G. *Z. Naturforsch.* **1982**, *A37*, 581.
(118) Caminiti, R.; Cucca, G.; Pintori, T. *Chem. Phys.* **1984**, *88*, 155.
(119) Licheri, G.; Paschina, G.; Piccaluga, G.; Pinna, G. *J. Chem. Phys.* **1984**, *81*, 6059.
(120) Ohtaki, H.; Yamaguchi, T.; Maeda, M. *Bull. Chem. Soc. Jpn.* **1976**, *49*, 701.
(121) Tajiri, Y.; Ichihashi, M.; Mibuchi, T.; Wakita, H. *Bull. Chem. Soc. Jpn.* **1986**, *59*, 1155.
(122) Ichihashi, M.; Wakita, H.; Masuda, I. *J. Solution Chem.* **1984**, *13*, 505.
(123) Magini, M.; Giubileo, G. *Gazz. Chim. Ital.* **1981**, *111*, 449.
(124) Magini, M. *J. Chem. Phys.* **1981**, *74*, 2523.
(125) Wertz, D. L.; Kruh, R. F. *Inorg. Chem.* **1970**, *9*, 595.
(126) Shapovalov, I. M.; Radchenko, I. V.; Lesovitskaya, M. K. *J. Struct. Chem.* **1972**, *13*, 121.
(127) Caminiti, R.; Cucca, P. *Chem. Phys. Lett.* **1982**, *89*, 110.
(128) Neilson, G. W.; Enderby, J. E. *Proc. R. Soc. London* **1983**, *A390*, 353.
(129) Enderby, J. E. *Pure Appl. Chem.* **1985**, *57*, 1025.
(130) Caminiti, R. *J. Chem. Phys.* **1982**, *77*, 5682.
(131) Licheri, G.; Pinna, G.; Navarra, G.; Vlaic, G. *Z. Naturforsch.* **1983**, *A38*, 559.
(132) Caminiti, R.; Licheri, G.; Piccaluga, G.; Pinna, G. *Faraday Discuss. Chem. Soc.* **1978**, *64*, 62.
(133) Neilson, G. W.; Enderby, J. E. *J. Phys. C: Solid State Phys.* **1978**, *11*, L625.
(134) Newsome, J. R.; Neilson, G. W.; Enderby, J. E.; Sandstrom, M. *Chem. Phys. Lett.* **1981**, *82*, 399.
(135) Magini, M.; DeMoraes, M.; Licheri, G.; Piccaluga, G. *J. Chem. Phys.* **1985**, *83*, 5797.
(136) Wakita, H.; Ichihashi, M.; Mibuchi, T.; Masuda, I. *Bull. Chem. Soc. Jpn.* **1982**, *55*, 817.
(137) Caminiti, R. *J. Chem. Phys.* **1986**, *84*, 3336.
(138) Sandstrom, D. R. *J. Chem. Phys.* **1979**, *71*, 2381.
(139) Sandstrom, D. R.; Dodgen, H. W.; Lytle, F. W. *J. Chem. Phys.* **1977**, *67*, 473.
(140) Caminiti, R.; Magini, M. *Chem. Phys. Lett.* **1979**, *61*, 40.
(141) Soper, A. K.; Neilson, G. W.; Enderby, J. E.; Howe, R. A. *J. Phys. C: Solid State Phys.* **1977**, *10*, 1793.
(142) Neilson, G. W. *J. Phys. C* **1982**, *15*, L233.
(143) Licheri, G.; Musinu, A.; Paschina, G.; Piccaluga, G.; Sedda, A. F. *J. Chem. Phys.* **1984**, *80*, 5308.
(144) Neilson, G. W. Private communication in: Enderby, J. E.; Neilson, G. W. *Rep. Prog. Phys.* **1981**, *44*, 593.
(145) Lagarde, P.; Fontaine, A.; Raoux, D.; Sadoc, A.; Migliardo, P. *J. Chem. Phys.* **1980**, *72*, 3061.
(146) Fontaine, A.; Lagarde, P.; Raoux, D.; Fontana, M. P.; Maisano, G.; Migliardo, P.; Wanderlingh, F. *Phys. Chem. Lett.* **1978**, *41*, 504.
(147) Ichihashi, M.; Wakita, H.; Mibuchi, T.; Masuda, I. *Bull. Chem. Soc. Jpn.* **1982**, *55*, 3160.
(148) Fishkis, M. Ya.; Zhmak, V. A. *J. Struct. Chem.* **1974**, *15*, 1.
(149) Ohtaki, H.; Maeda, M. *Bull. Chem. Soc. Jpn.* **1974**, *47*, 2197.
(150) Johansson, G.; Ohtaki, H. *Acta Chem. Scand.* **1973**, *27*, 643.
(151) Eisenberger, P.; Kincaid, B. M. *Chem. Phys. Lett.* **1975**, *36*, 134.
(152) Musinu, A.; Paschina, G.; Piccaluga, G.; Magini, M. *J. Appl. Crystallogr.* **1982**, *15*, 621.
(153) Radnai, T.; Palinkas, G.; Caminiti, R. *Z. Naturforsch.* **1982**, *A37*, 1247.
(154) Dagnall, S. P.; Hague, D. N.; Towl, A. D. C. *J. Chem. Soc., Faraday Trans. 2* **1982**, *78*, 2161.
(155) Wertz, D. L.; Bell, J. R. *J. Inorg. Nucl. Chem.* **1973**, *35*, 861.
(156) Musinu, A.; Paschina, G.; Piccaluga, G.; Magini, M. *J. Appl. Crystallogr.* **1982**, *15*, 621.
(157) Caminiti, R.; Johansson, G. *Acta Chem. Scand.* **1981**, *A35*, 373.
(158) Caminiti, R. *Z. Naturforsch.* **1981**, *A36*, 1062.
(159) Caminiti, R.; Cucca, P.; Radnai, T. *J. Phys. Chem.* **1984**, *88*, 2382.
(160) Caminiti, R.; Licheri, G.; Piccaluga, G.; Pinna, G. *Z. Naturforsch.* **1980**, *A35*, 1361.
(161) Ohtaki, H.; Maeda, M.; Ito, S. *Bull. Chem. Soc. Jpn.* **1974**, *47*, 2217.
(162) Sadoc, A.; Lagarde, P.; Vlaic, G. *J. Phys. C* **1985**, *18*, 23.
(163) van Eck, C. L. van P.; Wolters, H. B. M.; Jaspers, W. J. M. *Recl. Trav. Chim. Pays-Bas* **1956**, *75*, 802.
(164) Johansson, G. *Acta Chem. Scand.* **1971**, *25*, 2787.
(165) Sandstrom, M.; Persson, I.; Ahrland, S. *Acta Chem. Scand.* **1978**, *A32*, 607.
(166) Caminiti, R.; Licheri, G.; Piccaluga, G.; Pinna, G.; Radnai, T. *J. Chem. Phys.* **1979**, *71*, 2473.
(167) Caminiti, R.; Radnai, T. *Z. Naturforsch.* **1980**, *A35*, 1368.
(168) Bol, W.; Welzen, T. *Chem. Phys. Lett.* **1977**, *49*, 189.
(169) Johansson, G.; Wakita, H. *Inorg. Chem.* **1985**, *24*, 3047.
(170) Johansson, G.; Niinitso, L.; Wakita, H. *Acta Chem. Scand.* **1985**, *A39*, 359.
(171) Caminiti, R.; Licheri, G.; Piccaluga, G.; Pinna, G. *J. Chem. Phys.* **1976**, *65*, 3134.
(172) Caminiti, R. *Chem. Phys. Lett.* **1982**, *86*, 214.
(173) Caminiti, R.; Licheri, G.; Piccaluga, G.; Pinna, G. *J. Chem. Phys.* **1978**, *69*, 1.
(174) Caminiti, R.; Licheri, G.; Piccaluga, G.; Pinna, G. *Chem. Phys.* **1977**, *19*, 371.
(175) Cristini, A.; Licheri, G.; Piccaluga, G.; Pinna, G. *Chem. Phys. Lett.* **1974**, *24*, 289.
(176) Magini, M. *J. Chem. Phys.* **1980**, *73*, 2499.
(177) Lee, W. K.; Prohofsky, E. W. *J. Chem. Phys.* **1981**, *75*, 3040.
(178) Magini, M.; Caminiti, R. *J. Inorg. Nucl. Chem.* **1977**, *39*, 91.
(179) Magini, M.; Radnai, T. *J. Chem. Phys.* **1979**, *71*, 4255.
(180) Magini, M. *J. Chem. Phys.* **1979**, *70*, 317.
(181) Magini, M. *J. Inorg. Nucl. Chem.* **1978**, *40*, 43.
(182) Lind, M. D. *J. Chem. Phys.* **1967**, *46*, 2010.
(183) Caminiti, R.; Atzei, D.; Cucca, P.; Anedda, A.; Bongiovanni, G. *J. Phys. Chem.* **1986**, *90*, 238.
(184) Caminiti, R.; Paschina, G. *Chem. Phys. Lett.* **1981**, *82*, 487.
(185) Maeda, M.; Ohtaki, H. *Bull. Chem. Soc. Jpn.* **1977**, *50*, 1893.
(186) Tanaka, T.; Ogita, N.; Tamura, Y.; Okada, I.; Ohtaki, H.; Palinkas, G.; Spohr, E.; Heinzinger, K. *Z. Naturforsch.* **1987**, *A42*, 29.
(187) Glaser, J.; Johansson, G. *Acta Chem. Scand.* **1982**, *A36*, 125.
(188) Glaser, J. *Acta Crystallogr.* **1978**, *A34*, S197.
(189) Magini, M.; Cabrini, A.; Scibona, G.; Johansson, G.; Sandstrom, M. *Acta Chem. Scand.* **1976**, *A30*, 437.
(190) Smith, L. S.; Wertz, D. L. *J. Am. Chem. Soc.* **1975**, *97*, 2365. Smith, L. S.; McCain, D. C.; Wertz, D. L. *J. Am. Chem. Soc.* **1976**, *98*, 5125.
(191) Habenschuss, A.; Spedding, F. H. *J. Chem. Phys.* **1979**, *70*, 3758.
(192) Smith, L. S.; Wertz, D. L. *J. Inorg. Nucl. Chem.* **1977**, *39*, 95.
(193) Caminiti, R.; Cucca, P.; D'Andrea, A. *Z. Naturforsch.* **1983**, *A38*, 533.
(194) Narten, A. H.; Hahn, R. L. *Science (Washington, D.C.)* **1982**, *217*, 1249.
(195) Narten, A. H.; Hahn, R. L. *J. Phys. Chem.* **1983**, *87*, 3193.
(196) Steele, M. L.; Wertz, D. L. *Inorg. Chem.* **1977**, *16*, 1125.
(197) Ryss, A. I.; Levositskaya, M. K.; Shapovalov, I. M. *VINITI* **1976**, 856–76; *Chem. Abstr.* **1978**, *89*, 95116.
(198) Habenschuss, A.; Spedding, F. H. *J. Chem. Phys.* **1980**, *73*, 442.
(199) Steele, M. L.; Wertz, D. L. *J. Am. Chem. Soc.* **1976**, *98*, 4424.
(200) Habenschuss, A.; Spedding, F. H. *J. Chem. Phys.* **1979**, *70*, 2797.
(201) Annis, B. K.; Hahn, R. L.; Narten, A. H. *J. Chem. Phys.* **1985**, *82*, 2086.
(202) Brady, G. W. *J. Chem. Phys.* **1960**, *33*, 1079. (a) Marcus, Y. In *Gmelin Handbook of Inorganic Chemistry, Rare Earths* **1981**, *Suppl. Vol. D3*, 1.
(203) Narten, A. H. *J. Phys. Chem.* **1970**, *74*, 765.
(204) Copestake, A. P.; Neilson, G. W.; Enderby, J. E. *J. Phys. C* **1985**, *18*, 4211.

(205) Lee, S. C.; Kaplow, R. *Science* (*Washington, D.C.*) **1970**, *169*, 477.
(206) Triolo, R.; Narten, A. H. *J. Chem. Phys.* **1975**, *63*, 3624.
(207) Cummings, S.; Enderby, J. E.; Neilson, G. W.; Newsome, J. R.; Howe, R. A.; Howells, W. S.; Soper, A. K. *Nature* (*London*) **1980**, *287*, 714.
(208) Brady, G. W.; Krause, J. T. *J. Chem. Phys.* **1957**, *27*, 304.
(209) Biggin, S.; Enderby, J. E.; Hahn, R. L.; Narten, A. H. *J. Phys. Chem.* **1984**, *88*, 3634.
(210) Neilson, G. W.; Schioberg, D.; Luck, W. A. P. *Chem. Phys. Lett.* **1985**, *122*, 475.
(211) Neilson, G. W.; Enderby, J. E. *J. Phys. C: Solid State Phys.* **1982**, *15*, 2347.
(212) Caminiti, R.; Licheri, G.; Piccaluga, G.; Pinna, G. *J. Chem. Phys.* **1978**, *68*, 1967.
(213) Caminiti, R.; Cucca, P.; Atzei, D. *J. Phys. Chem.* **1985**, *89*, 1457.
(214) Caminiti, R.; Paschina, G.; Pinna, G.; Magini, M. *Chem. Phys. Lett.* **1979**, *64*, 391.
(215) Johansson, G.; Caminiti, R. *Z. Naturforsch.* **1986**, *A41*, 1325.
(216) Hajdu, F.; Lengyel, S.; Palinkas, G. *J. Appl. Crystallogr.* **1976**, *9*, 134.
(217) Kalman, E.; Palinkas, G.; Kovacs, P. *Mol. Phys.* **1977**, *34*, 505, 525.
(218) Thiessen, W. E.; Narten, A. H. *J. Chem. Phys.* **1982**, *77*, 2656.
(219) Gibson, I. P.; Dore, J. C. *Mol. Phys.* **1983**, *48*, 1019.
(220) Impey, R. W.; Klein, M. L.; McDonald, I. R. *J. Chem. Phys.* **1981**, *74*, 647.
(221) Desnoyers, J. E.; Verall, R. E.; Conway, B. E. *J. Chem. Phys.* **1965**, *43*, 243.
(222) Jansco, G.; Bopp, P.; Heinzinger, K. *Chem. Phys.* **1984**, *85*, 377.
(223) Gaballa, G. A.; Neilson, G. W. *Mol. Phys.* **1983**, *50*, 97.
(224) Deraman, M.; Dore, J. C.; Powles, J. G.; Holloway, J. H.; Chieux, P. *Mol. Phys.* **1985**, *55*, 1351.
(225) McDonald, I. R.; Klein, M. L. *J. Chem. Phys.* **1976**, *64*, 4790.
(226) Chieux, P.; Bertagnolli, H. *J. Phys. Chem.* **1984**, *88*, 3726.
(227) Narten, A. H. *J. Chem. Phys.* **1977**, *66*, 3117.
(228) DeSando, R. J.; Brown, G. H. *J. Phys. Chem.* **1968**, *72*, 1088.
(229) Kalman, E.; Serke, I.; Palinkas, G.; Zeidler, M. D.; Wiesmann, F. J.; Bertagnolli, H.; Chieux, P. *Z. Naturforsch.* **1983**, *A38*, 231.
(230) Ohtaki, H.; Funaki, A.; Rode, B. M.; Reibnegger, G. J. *Bull. Chem. Soc. Jpn.* **1983**, *56*, 2116.
(231) Miyake, M.; Kaji, O.; Nakagawa, N.; Suzuki, T. *J. Chem. Soc., Faraday Trans. 2* **1985**, *81*, 277.
(232) Ohtaki, H.; Itoh, S. *Z. Naturforsch.* **1985**, *A40*, 1351.
(233) Ohtaki, H.; Itoh, S.; Rode, B. M. *Bull. Chem. Soc. Jpn.* **1986**, *59*, 271.
(234) Ohtaki, H.; Itoh, S.; Yamaguchi, T.; Ishiguro, S.; Rode, B. M. *Bull. Chem. Soc. Jpn.* **1983**, *56*, 3406.
(235) Jorgensen, W. L. *J. Am. Chem. Soc.* **1981**, *103*, 341, 345.
(236) Jorgensen, W. L.; Ibrahim, M. *J. Am. Chem. Soc.* **1982**, *104*, 373.
(237) Magini, M.; Paschina, G.; Piccaluga, G. *J. Chem. Phys.* **1982**, *77*, 2051.
(238) Narten, A. H.; Habenschuss, A. *J. Chem. Phys.* **1984**, *80*, 3387.
(239) Tanaka, Y.; Ohtomo, N.; Arakawa, K. *Bull. Chem. Soc. Jpn.* **1985**, *58*, 270.
(240) Narten, A. H.; Sandler, S. I. *J. Chem. Phys.* **1979**, *71*, 2069.
(241) Bertagnolli, H.; Chieux, P.; Hertz, H. G. *Ber. Bunsenges. Phys. Chem.* **1984**, *88*, 977.
(242) Kratochwill, A.; Weidner, J. U.; Zimmermann, H. *Ber. Bunsenges. Phys. Chem.* **1973**, *77*, 408.
(243) Acrivos, J. V.; Hathaway, K.; Robertson, A.; Thompson, A.; Klein, M. P. *J. Phys. Chem.* **1980**, *84*, 1206.
(244) Lelieur, J. P.; Goulon, J.; Cortes, R.; Friant, P. *J. Phys. Chem.* **1984**, *88*, 3730.
(245) Tanabe, Y.; Rode, B. M. *Abstr. VIII Int. Symp. Solute–Solute–Solvent Interact., Regensburg, 1987*; Barthel, J., Schmeer, G., Eds.; p P1.06.
(246) Ohtaki, H.; Wada, H. *J. Solution Chem.* **1985**, *14*, 209.
(247) Kabisch, G.; Kalman, E.; Palinkas, G.; Radnai, T.; Gaizer, F. *Chem. Phys. Lett.* **1984**, *107*, 463.
(248) Sandstrom, M.; Persson, I.; Ahrland, S. *Acta Chem. Scand.* **1978**, *A32*, 607.
(249) Ohtaki, H. *Pure Appl. Chem.* **1987**, *59*, 1143.
(250) Sano, M.; Maruo, T.; Yamatera, H. *J. Chem. Phys.* **1986**, *84*, 66.
(251) Wertz, D. L.; Lawrence, R. M.; Kruh, R. F. *J. Chem. Phys.* **1965**, *43*, 2163.
(252) Wertz, D. L.; Kruh, R. F. *J. Chem. Phys.* **1969**, *50*, 4013.
(253) Jorgensen, W. L.; Bigot, B.; Chandrasekhar, J. *J. Am. Chem. Soc.* **1982**, *104*, 4584.
(254) Ichihashi, M.; Wakita, H.; Masuda, I. *Bull. Chem. Soc. Jpn.* **1983**, *56*, 3761.
(255) Radnai, T.; Kalman, E.; Pollmer, K. *Z. Naturforsch.* **1984**, *A39*, 464.
(256) Sano, M.; Maruo, T.; Masuda, Y.; Yamatera, H. *J. Solution Chem.* **1986**, *15*, 803.
(257) Ergin, Yu. V.; Koop, O. Ya.; Khrapko, A. M. *Zh. Fiz. Khim.* **1981**, *55*, 173; *Russ. J. Phys. Chem.* (*Engl. Transl.*) **1981**, *55*, 90.
(258) Marchese, F. T.; Beveridge, D. L. *Int. J. Quant. Chem.* **1986**, *29*, 619.
(259) Jansco, G.; Heinzinger, K.; Radnai, T. *Chem. Phys. Lett.* **1984**, *110*, 196.